THE UNIVERSITY OF BIRMINGHAM

MRes Research Project 1

Molecular interactions of AMIGO family members

737539

8/15/2011

THE UNIVERSITY
OF BIRMINGHAM

Contents

MRes Research Project 2

Figure listings.

Abstract.

The regenerative capacities between the peripheral and central nervous systems are contrasting; with axons in the peripheral nervous system being able to regenerate, unlike those in the central nervous system (CNS). Upon injury, the CNS responds by releasing myelin breakdown products, which are inhibitory to axon regrowth, and the formation of the glial scar which forms a physical barrier to regeneration. Whilst the formation of the glial scar takes days or weeks to form, the myelin breakdown products, which include myelin associated glycoprotein (MAG), oligodendrocyte myelin glycoprotein (OMgp) and Nogo, exert their inhibitory effects immediately. These products bind to the Nogo Receptor (NgR) complex which consists of the Nogo receptor (NgR), p75 neurotrophin receptor ($p75^{NTR}$)/ (or an alternative protein known as TROY) and Lingo-1 which work together to activate RhoA, resulting in actin depolymerisation and growth cone collapse. The specific mechanisms by which this complex exhibits its effects remain unclear, particularly as recent unpublished data suggest that specific members of the Amigo family of proteins may be critical mediators of the inhibitory signaling pathway in *vivo*. This suggestion prompted us to clone NgR, $p75^{NTR}$ and Amigos 1, 2 and 3 in mammalian expression vectors and perform co-immunoprecipitation experiments with these constructs. These experiments suggest that Amigo-1 and -3 bind to NgR and/or $p75^{NTR}$ both independently or when expressed together. Although the approach was only semiquantitative at best, the experiments also suggest that Amigo 2 may bind to NgR and $p75^{NTR}$ independently and together, but to a much lesser extent. The results indicate that the Amigo family of proteins may form a component of the axon growth inhibitory complex, and potentially forming novel therapeutic targets for CNS injury.

Acknowledgements.

I would like to thank Dr's Michael Douglas and Ben Willcox as well as everyone in the Willcox group for their help throughout my 12 week project.

1. Introduction

It has long been known that there is a difference in the regenerative capacities between the central nervous system (CNS) and peripheral nervous system (PNS). In common with most tissues, axons in the PNS are generally able to regenerate successfully after injury, whilst those in the CNS exhibit limited regeneration at best. A consequence of this is that functional recovery after CNS injury or disease is rare. The biochemical and cellular mechanisms underlying these differences are likely to be multifactorial, and are a subject of substantial interest because understanding them could lead to new therapeutic opportunities to enhance regeneration of axons after tissue injury or in diseases. After damage occurs to the CNS it undergoes an injury response which involves a series of events evolving over several days and weeks [1]. These include the release of myelin breakdown products and the subsequent formation of a glial scar, two phenomena acting to prevent regeneration of damaged axons [2]. Damage to myelin occurs early following injury, leading to the local release of inhibitory factors including myelin associated glycoprotein (MAG), oligodendrocyte myelin glycoprotein (OMgp) and Nogo. Therefore these myelin breakdown products play a critical role in preventing neuronal regeneration but currently their mechanisms remain unclear. In contrast to the rapid release of myelin derived inhibitors, the glial scar is established over weeks as a meshwork of reactive astrocytes, oligodendrocyte precursors, and microglia that may form a physical barrier to regeneration [3]. Astrocytes within the glial scar also upregulate the production of several extracellular matrix associated inhibitors of regeneration [2] including chondroitin sulphate proteoglycans (CSPGs) which are important in the development and maintenance of the normal CNS, but are also the main inhibitory molecules to axon regeneration in the glial scar [4]. Evidence that CSPGs are inhibitory to axon regeneration comes from research

showing that levels of CSPGs are elevated around CNS injuries [1] and that axon regeneration stops around the area that these CSPGs accumulate. CSPGs are detected a few days after injury to the CNS and remain for several weeks after making the environment around the site of injury hostile to axonal survival and growth for a considerable period.

It is widely acknowledged that the inhibitory signals transmitted to neurons in the early stage of the inhibitory process mediated by myelin breakdown products play a critical role in establishing the inhibitory effects of the glial scar and CSPGs. Affecting this early stage inhibitory signal provided by the release of these products, prior to the formation of the glial scar and CSPGs are released, would be critical to the success of therapeutic interventions aimed at promoting CNS regeneration following injury.

1.1. MAG

Immediately following CNS injury which causes damage to myelin, debris containing inhibitory proteins is released. These proteins are removed very slowly from the site of injury due to the low phagocytic activity in this area. These myelin derived inhibitory proteins include MAG, OMgp and Nogo. Myelin associated glycoprotein (MAG) is produced by oligodendrocytes, and has roles in axon stability, controlling axon cytoarchitecture and regulating axon outgrowth [5]. MAG is a sialic acid binding- SIGLEC (sialic acid- dependent immunoglobulin- like family member lectin) protein [6] which binds to gangliosides GD1a and GT1b on nerve cells and axons [5]. MAG has also been found to be a ligand for the Nogo receptor (NgR), which it binds to with high affinity. MAG seems to have a complex function, inhibiting specific axon growth pathways, also

MAG knockout mice only display a limited enhancement of axon regeneration in the CNS. So whilst it is clear that MAG has inhibitory roles in axon regeneration in the CNS it is also clear that there are other inhibitory proteins present.

1.2. OMgp

Oligodendrocyte myelin protein (OMgp) is a glycosylphosphatidylinositol (GPI) anchored protein present on the surface of oligodendrocytes and myelin surfaces adjacent to axons. It was found to be inhibitory to axon regrowth when myelin fractions were tested for inhibitory activity [7]. OMgp has been found to cause growth cone collapse in vitro but its function *in vivo* is not yet known [8].

1.3. Nogo

Early experiments (Caroni et al. 1988, Schwab and Caroni 1988) found that a 250kDa protein extracted from myelin was responsible for inhibiting neurite outgrowth; this was termed NI-250. An antibody called 1N-1 was raised against this protein which blocked the inhibitory activity of this protein which was subsequently named Nogo.

Nogo belongs to the Reticulon (RTN) family of proteins which are a large group of membrane-associated proteins present in all eukaryotic organisms [9]. There are four different RTN genes with Nogo classified as RTN 4. Additionally, there are 3 isoforms of Nogo known as Nogo-A, -B and –C which are generated by alternative promotor usage and/or splicing from a single RTN4 gene [10]. The proteins share a 188 amino acid domain in their C terminal regions, known as the reticulon homology domain (RHD)

which is highly conserved between RTN protein members [10]. The RHD is composed of two membrane spanning hydrophobic stretches [11] which are separated by a 66 residue hydophillic segment, a domain conserved throughout the three isoforms of Nogo, whereas the amino terminal regions, dervived from alternative RNA splicing events, are not structurally related [12]. The topology of Nogo is unusual, with the N terminus and C terminus cytosolic and the short 66 amino acid axon inhibitory loop protruding into the luminal or extracellular space [13].

Nogo-A is the longest isoform of Nogo and is highly expressed in oligodendrocytes but not in Schwann cells [14] ,consistent with finding that Nogo-A is a major CNS myelin associated inhibitor. Nogo-B and Nogo-C have not been identified in myelin-forming oligodendrocytes and so most studies to date have focussed on Nogo-A [14]. Expression levels are dynamic - , with Nogo-A expression levels increased after trauma [15]. Nogo-A is principally expressed in the endoplasmic reticulum, in a finely granulated pattern, with a small amount been expressed at the cell surface [12]. So far two regions have been identified on this protein that have a negative affect on the regeneration of neurons, the first being common to all three isoforms - an extracelular 66 amino acid domain located next to the C terminal known as Nogo 66. The second inhibitory domain on Nogo-A is a region located in its N terminus - known as amino Nogo. This latter domain is intracellular and has actions that are not cell type specific [16]. These two domains on the Nogo-A protein may act synergistically to inhibit neurite outgrowth in the injured CNS [16].

1.4. Nogo Receptor (NgR)

Although two inhibitory domains have been described for Nogo-A, only one receptor has been identified so far [17], binding the Nogo-66 domain of Nogo-A with high affinity and is therefore known as the Nogo-66 receptor, NgR. This receptor mediates the inhibition of axonal regeneration caused by Nogo-66 and it has been shown that expression of the receptor is sufficient to convert axonal growth cones from Nogo-66 insensitive to Nogo-66 responsive [16]. The NgR is part of a family of three glycosylphosphatidylinositol (GPI) anchored proteins, called NgR-1,-2 and -3. NgR1 is known to interact not only with Nogo-66 but also MAG and OMgp [18] which also act to suppress neurite outgrowth. Cleavage of NgR from the cell surface also renders axons insensitive to these ligands [3]. This observation is very remarkable as there is no sequence similarity between these NgR ligands [19].

The NgR is predicted to contain 473 amino acids [14] and is detectable as a ~85kDa band following denaturing SDS-PAGE [20]. In addition to a GPI anchor, it contains eight leucine rich repeats (LRRs), flanked by a cysteine-rich C terminal subdomain (LRRCT) and by a smaller leucine-rich N terminal domain (LRRNT) [19].

NgR mRNA is expressed selectively in adult neurons [21], and the corresponding NgR proteins are found throughout axons in the adult and maturing CNS in a distribution in which they may receive signals from Nogo proteins. This matched distribution contrasts with MAG and OMgp which are expressed in many tissues where there is little or no NgR expression [21]. This suggests that, along with interacting with NgR to inhibit axonal

growth, MAG and OMgp, may have other roles and act on other receptors. Supporting this, it has been found that genetic deletion of NgR has only shown moderate disinhibitory effects suggesting that other receptors for Nogo, MAG and OMgp exist. Atwal et al. [22] found that paired immunoglobulin like receptor B (PIR-B), a type1 transmembrane glycoprotein, binds these ligands with high affinity, they also found that blocking this receptor partially rescues the neurite inhibition from Nogo, MAG, OMgp and that blocking both the PIR-B and the NgR receptors enables almost complete release from myelin inhibition. This group suggest that PIR-B may even be a more important factor in axonal growth inhibition than NgR as deletion of PIR-B resulted in greater neurite outgrowth than that achieved by deletion of NgR. The fact that these structurally unrelated receptors can both bind three structurally unrelated ligands with high affinity highlights key complexities in the regulation of CNS tissue regeneration.

1.5. $p75^{NTR}$

Since NgR is GPI anchored and lacks a cytoplasmic domain, the entire protein mass is located on the extracellular side of the membrane and therefore requires a transmembrane co-receptor to direct signal transduction into the cell. Wang et al [23] demonstrated that the molecule responsible for the transduction of inhibitory signals is a member of the TNF receptor family- the p75 neurotrophin receptor ($p7^{5NTR}$) [23], it was found that the $p75^{NTR}$ specifically binds to NgR and is necessary for NgR mediated signalling. Furthermore, blocking experiments between NgR and $p75^{NTR}$ caused a reduction in the inhibitory activities of Nogo, MAG and OMgp.

The $p75^{NTR}$ - receptor is a 399 amino acid type 1 transmembrane protein, expressed in a wide variety of cells in the CNS during development. $p75^{NTR}$ was originally identified as a neurotrophin binding receptor, with dynamic expression levels, declining to background levels in the adult CNS, but upregulated following CNS injury. Neurotrophins are growth factors and include nerve growth factor (NGF), brain derived growth factor (BDGF) and neurotrophins 3, 4 and 5 secreted by sympathetic and sensory target organs as well as neurons and provide support to neurons as they reach their final target [24]. In a similar manner to $p75^{NTR}$, neurotrophin production increases after injury to the nervous system [25]. When acting as an inhibitory mediator, the NgR/$p75^{NTR}$ complex is activated by Nogo, MAG or OMgp, and $p75^{NTR}$ acts as to release the small GTP binding protein RhoA, resulting in actin depolymerisation and growth cone collapse [26].

The importance of $p75^{NTR}$ in the formation of an active inhibitory receptor complex has been shown in many studies. Studies have shown that the extracellular domain of $p75^{NTR}$ is necessary for its binding to NgR, whereas its intracellular and transmembrane regions are not necessary [23]. This study also demonstrated that blocking association of the extracellular region of $p75^{NTR}$ with NgR inhibited the effects of the myelin breakdown products MAG, OMgp and Nogo-66. The intracellular domain was found to be necessary for transduction of the inhibitory signal across the membrane, as a truncated form of the receptor allowed robust neurite outgrowth [23]. Although $p75^{NTR}$ has been shown to be an important factor in the inhibition of neurite outgrowth *in vitro*, its exact role is not fully established *in vivo*, not least because the tissue distribution of NgR does not correspond well to the distribution of $p75^{NTR}$, and $p75^{NTR}$ is not ubiquitously expressed in the adult brain where all the neurons are responsive to myelin inhibition [27]. Also, whilst $p75^{NTR}$ negative mice do not show RhoA activation or neurite outgrowth inhibition, when $p75^{NTR}$

is co-expressed with NgR in non neuronal cells there was no activation of RhoA [28] in response to myelin breakdown products suggesting that although $p75^{NTR}$ is necessary for the negative regulation of neurite outgrowth, other components must be involved too.

1.6. TROY

As $p75^{NTR}$ is not widely expressed in the adult CNS, and CNS neurons are still inhibited by myelin breakdown products, it was postulated that there might be a functional homologue of $p75^{NTR}$ that is more widely expressed in the adult CNS that would substitute $p75^{NTR}$ in the NgR complex. These considerations led to the discovery of TROY, a member of the TNF receptor family, could bind to NgR with high affinity [29], and activates RhoA in response to myelin breakdown products. Unlike $p75^{NTR}$, TROY is broadly expressed in the CNS, leading the authors to conclude that TROY can substitute for $p75^{NTR}$ in the inhibitory receptor complex in the adult CNS.

1.7. Lingo 1

Lingo (LRR and Ig domain –containing, Nogo receptor-interacting protein) 1 was identified as a member of the inhibitory receptor complex, transducing signals across the membrane and is an important negative regulator of oligodendrocyte differentiation [30]. Lingo1 is a 614 amino acid protein [31] containing 12 leucine rich repeats which are flanked by a C- and N- terminal (LRRCT and LRRNT). The C-terminal region is composed of an immunoglobulin (Ig) domain, a transmembrane domain and a short cytoplasmic tail. Lingo-1 is a member of the LRRIg family of proteins which all contain leucine rich repeats (LRR) and immunoglobulin (Ig) domains, with several members involved in central nervous system development. Lingo1 has been shown to be present on

neural but not in non neural tissues, with highest expression levels found in the cortex [28]. Like $p75^{NTR}$, Lingo1 expression is highest during embryogenesis and decreases thereafter to very low levels in adulthood.

Lingo1 acts as an accessory molecule which acts to structurally and functionally stabilise the NgR/$p75^{NTR}$ inhibitory complex, The *in vitro* actions of Lingo-1 have been examined in detail by Ji, B et al [32] who blocked Lingo-1 binding to NgR with a Lingo-1-Fc antagonist. The outcome was a significantly improved functional recovery, axonal sprouting and a decrease in RhoA activation, with similar *in vitro* results obtained by Mi, S et al 2004 [28]. However the functional significance of Lingo1 has not been demonstrated *in vivo*, with Lingo 1 antagonism resulting in only a very small difference in axonal sprouting, leading to the idea that more molecules may substitute for Lingo 1 in the inhibitory process.

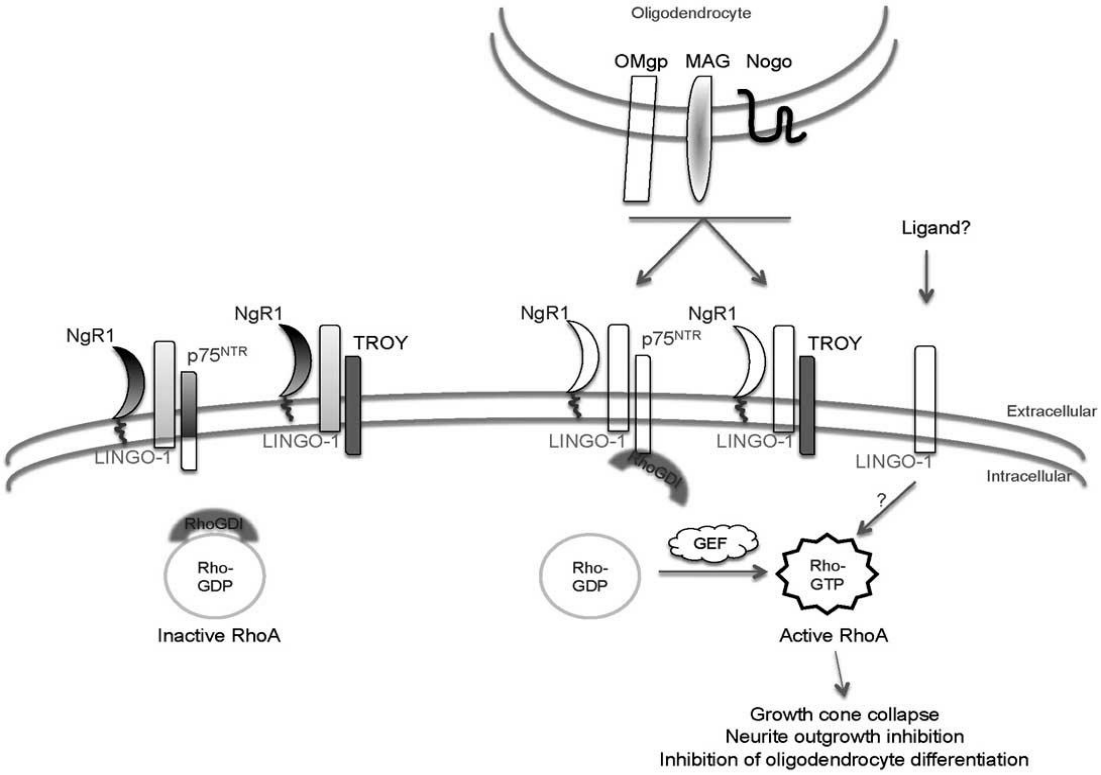

Figure 1.1. Diagram showing the relationship between the various components involved in inhibition of axonal regeneration.

The Nogo-66 protein acts on the NgR which forms a complex with $p75^{NTR}$ or Troy and Lingo1 which act together to activate RhoA which results in an inhibition of growth. [3].

1.8. An array based approach to identification of key components of the NgR complex.

In a series of unpublished experiments (M Douglas, personal communication), researchers in the Molecular Neuroscience Group (University of Birmingham) performed a series of microarray experiments detailing gene expression profiles in a series of rat CNS injury

models. Amongst numerous differentially modulated genes, the gene for LRRIg receptor AMIGO3 was observed to be upregulated following traumatic injury. Of particular interest, the gene was additionally found to be downregulated in a modified CNS injury paradigm associated with axon regeneration. Subsequent results found that the addition of siRNA to AMIGO3 to *in vitro* cultures of dissociated dorsal root ganglia permitted neurite growth under otherwise growth inhibitory conditions. Collectively these data suggest a potential function for Amigo3 in the transmission of neuronal inhibitory signals after injury, but did not establish a molecular mechanism and suggesting further research was needed looking into the role of Amigo3 and the Amigo family of proteins in the formation and function of the NgR complex.

1.9. Amigo

The Amigo family of proteins, a subset of closely related LRRIg receptors, were first identified in experiments investigating the transcriptional effects of a protein called amphoterin, known to promote cell motility and neurite outgrowth. Expression of the amigo gene was induced by amphoterin giving it its name -Amphoterin induced gene and ORF (Amigo). Amphoterin, also known as HMGB1, is a heparin binding protein acting as a ligand for the receptor for advanced glycation end products (RAGE), initially discovered in rat brain but also subsequently identified in many cell types including fibroblasts [33].

The Amigos are members of the LRRIg family of proteins of which Lingo1 is a member, and therefore contain both leucine rich repeats (LRR) and immunoglobulin (Ig) domains. Their LRRs are normally 20-29 amino acids long and consist of a beta sheet and a helix connected by loops, forming a curved horseshoe shaped structure [34]. Leucine rich

repeats are found in a large number of proteins and act as interaction motifs. The domain arrangement consists of a type 1 transmembrane protein which containing six LRRs flanked by cysteine rich LRR -C and -N (LRRCT and LRRNT) terminals and an Ig domain close to the transmembrane region [35]. Further experiments functionally characterised the Amigo proteins, suggesting that the Amigo family manifest both homophillic and heterophilic binding properties.

Individual amigo proteins are differentially expressed in tissues, with Amigo 1 mostly restricted to central nervous system tissues (cerebrum, cerebellum and the retina), whilst Amigo 2 and Amigo 3 expression was much more widespread (Fig.1.2). Amigo 2 was found to be expressed mostly in the cerebellum, retina, liver and lung with lower amounts found in other tissues and Amigo3 was shown to be expressed in all tissues tested in the study [35].

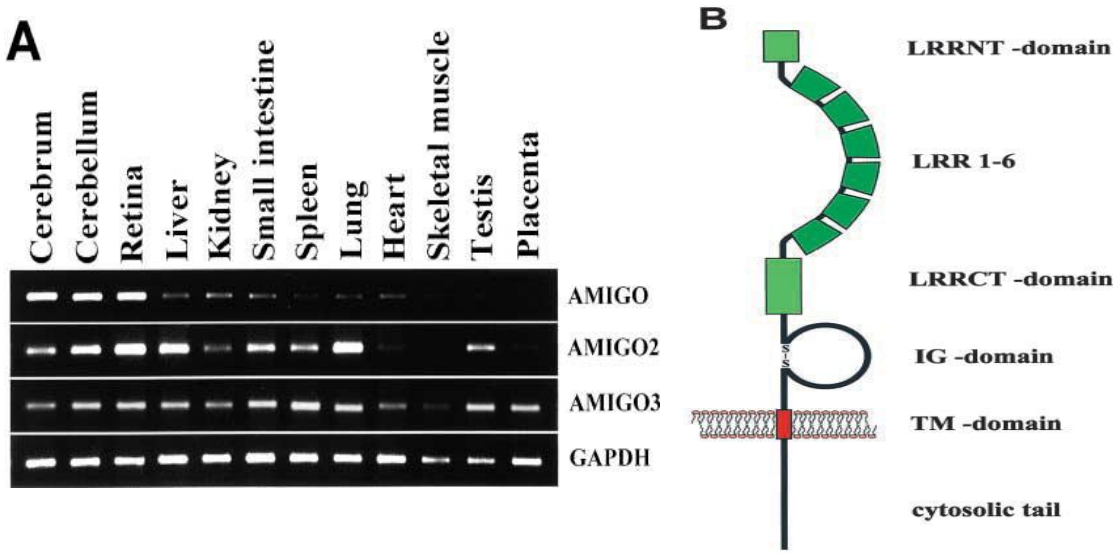

Figure 1.2. Location and structure of the Amigo proteins.

a) The Amigo proteins have differing distributions with the body, whilst Amigo1 is almost exclusively expressed in the central nervous system, Amigo2 and Amigo3 are more widespread [35].

b) The Amigo proteins are made up of 6 leucine rich repeats (LRR) flanked by leucine rich N and C terminal domains, with an Ig domain close to the cell membrane followed by the transmembrane region and a short cytoplasmic tail [35].

1.10. Hypothesis

Research to date suggests that axon inhibitory signaling pathways are dependent on the formation of a trimeric complex, consisting principally of NgR, $p75^{NTR}$ and Lingo-1. The functional significance of this specific protein arrangement *in vivo* is unclear, however, a range of potential binding partners from the LRRIg family of proteins may substitute for components of this complex. This leads us to propose the hypothesis that members of the Amigo family of proteins may act as binding partners for NgR and/or $p75^{NTR}$, substituting for Lingo-1 in the formation of an inhibitory signaling complex.

1.11. Aims

The project aims firstly, to clone human full length versions of NgR, $p75^{NTR}$, Lingo1 and Amigo 1 to 3. Following this, these constructs will then be transiently expressed in mammalian cells, with the resulting proteins used in co- immunoprecipitation experiments to determine their relative binding specificities.

2. Materials and Methods

2.1. Materials

Plasmids

cDNA constructs were cloned into the expression vector pAAV-IRES-hrGFP (Stratagene). The vector contains an ampicillin resistance gene to allow antibiotic selection in bacteria, a CMV promoter for gene expression in mammalian cells and a multiple cloning site (MCS) followed by three tandem 3' FLAG tag sequences. In addition, a hrGFP gene allows visualisation of transfected cells.

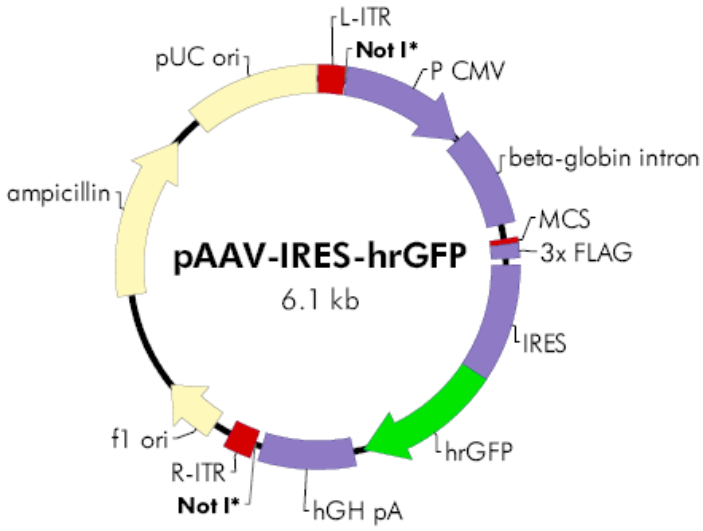

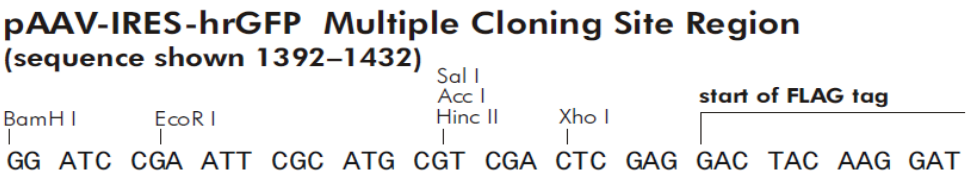

Figure 2.1. Plasmid map and multiple cloning site of pAAV-IRES-hrGFP.

The vector map shows the position of the 3x FLAG tag after the multiple cloning site.

2.2. Methods

PCR

Polymerase chain reaction (PCR) was used to amplify Amigo1, Amigo2, Amigo3, and p75 cDNA which had been obtained from GeneService and Lingo 1 and NgR cDNA which had been obtained from Thermo Scientific. The designed primers (detailed in the appendix) incorporated either 5' EcoRI or BamHI sites and a 3' XhoI restriction site to allow incorporation into pAAV-IRES-hrGFP cut with the corresponding enzymes. Stop signal codons were removed where desired, to produce a 3' fusion with the tandem FLAG sequences from the plasmid vector. PCR reactions were performed using an ABI 9600 thermal cycler with the following cycling conditions: an initial denaturation step of 96^{o}C, followed by 18 cycles of 96^{o}C for 30 seconds/55^{o}C for 30 seconds/72^{o}C for 90 seconds. A final 5 minute 72^{o}C extension was used to complete the reactions. Amplification was carried out using either the Expand High Fidelity enzyme (Roche) or Pfu Turbo enzyme (Agilent).

Typically, PCR reactions were prepared as follows:

0.5-1µl Template DNA

2µl forward and reverse primers at a concentration of 20pm/µl each

1µl deoxynucleotide triphosphates (dNTPs) at a concentration of 10mM

5µl of PCR buffer (10x)

38-38.5µl H_20 (up to 50µl)

1µl PCR Enzyme

Overlap extension PCR

Overlap extension reaction PCR was performed to perform either site directed mutagenesis or fuse cDNA sequences to create chimeric gene sequences. The approach uses a two step PCR reaction – in the first set of reactions, two PCR products are created – the 5' product (A), using an external forward primer and an internal reverse primer, and 3' product (B), using an internal forward primer and an external reverse primer. Each internal primer is designed to produce a mutually complimentary overlapping region of 36 base pairs. In the second reaction, the two PCR products are fused by using a mixture of (A) and (B) as templates, using the external primers only to create a single product (A+B). The mutated or chimeric product (A+B) is then cloned using standard techniques.

Agarose Gel Electrophoresis

Agarose gel electrophoresis was used to separate DNA fragments according to their length, with electrophoresis in 1% agarose gels in TAE, with 0.5µg/ml ethidium bromide added to allow visualisation of the DNA bands. Electrophoresis was performed using a current of 80mA until clear separation of PCR products was observed. Sizing of PCR products was demonstrated using DNA ladders appropriate to their size, including the 100bp (Roche) and 1Kb DNA ladders (Fermentas/ Invitrogen). PCR products were visualised under a low level UV light source and appropriate bands excised.

Gel Purification

Excised DNA bands were purified using Qiaquick spin columns (Qiagen) based on the standard spin protocol. The purified DNA was eluted into 30µl of elution buffer and stored at -20^{o}C until required.

Restriction Digests

Purified DNA was digested with relevant restriction enzymes (NEB), with restriction digests typically set up using 30µl of purified DNA, 4µl of appropriate NEB digestion buffer, 2µl of enzyme 1 (EcoRI or BamHI) and 2µl of enzyme 2 (XhoI) and 2µl of H_20 for a total reaction volume of 40µl. Digests were performed at 37^oC and incubated for 2 hrs. pAAV-IRES-hrGFP plasmid was similarly digested with appropriate enzymes, purified and stored at -20^oC.

Ligation

DNA inserts were ligated into cut pAAV-IRES-hrGFP vectors under varying conditions ranging from room temperature for 1hr to 20°C overnight. The quantity of insert DNA required for the ligation reactions was determined by visualising levels of DNA and comparing against a known standard using agarose gel electrophoresis. The ligation reaction typically consisted of 2-5 µl insert DNA, 0.5-1µl of vector, 1µl of T4 DNA ligase enzyme, 1µl (10x) ligase buffer and H_20 to a final volume of 10µl.

Transformation

Ligation mixes were transformed into chemically competent Top10 *E.coli* (Invitrogen) via heat shock treatment. Cells were thawed on ice, following which 4µl of the ligated vector mix was added. After 30 minutes on ice the cells were heat shocked at 42^oC for 30 seconds before being placed back on ice for 2 minutes, following which 250µl of rich growth media SOC was added. The cells were incubated in an orbital shaker at 37^oC for

1hr at 220 rpm before being plated onto LB/agar plates containing 100ug/ml ampicillin and incubated overnight at 37^{o}C.

Plasmid Mini Prep

Single bacterial colonies were inoculated into 5mls of LB containing 100ug/ml ampicillin and incubated overnight at 37^{o}C in an orbital shaker at 220 rpm. 3ml of the 5ml culture was centrifuged and from the resulting pellet, plasmid DNA was extracted using a Qiagen Mini Prep kit, following the mini spin protocol. DNA was eluted into 50µl of elution buffer (50 mM Tris pH 7.5) and stored at -20^{o}C.

PCR Screening

Mini prep DNA was analysed by PCR to verify whether the gene of interest had been transformed successfully. For the PCR screening process, 2xBioMix (Bioline) was used which contains a 2x mix of Taq DNA polymerase enzyme, enzyme buffer and dNTPs. PCR reactions were set up as follows:

1µl plasmid DNA

2µl forward and reverse primers

20µl BioMix (2x)

15µl H_2O

An initial denaturation step of 96^{o}C was used, followed by 18 cycles of 96^{o}C for 30 seconds/55^{o}C for 30 seconds/72^{o}C for 90 seconds. After the reaction had finished 10µl of the PCR mix were run on a 1% agarose gel. The gel was viewed under UV light to determine which clones contained the insert.

DNA Sequencing

DNA sequencing was used to ascertain if any mutations were introduced into the DNA during the PCR and cloning process. Sequencing reactions were set up by adding 7µl of the mini prep DNA to 7µl of H_2O and adding 1µl of the appropriate sequencing primer (final primer concentration 3.5 pmol). To ensure full coverage of cloned inserts, three primers were used, the first being a Beta globulin primer, priming for the 5' region of the insert, followed by two internal primers at appropriate intervals (designed internal primer sequences in the appendix). Sequences were analysed using Sequencher software.

DNA Midi Prep

Midi scale DNA preparations were performed to produce sufficient quantities for eukaryotic cell transfection. A single colony was picked from a cloning plate, and grown in 100ml of LB/ampicillin (100ug/ml) overnight at 37^{o}C. DNA was purified using NucleoBond Xtra Midi columns (Clontech) according to standard protocols. Following the purification steps the DNA was eluted into 5ml of elution buffer then precipitated with isopropanol, 70% ethanol and finally resuspended into 100µl of 50 mM Tris pH 7.5.

DNA quantification

DNA obtained from the midi preparations was quantified using nanodrop apparatus (Thermo scientific) using absorbance readings at 260 nm. 1.5µl samples were analysed, using H_20 as a blank. Resulting DNA concentrations were calculated in ng/µl and samples were normalised to a final concentration of 1000 ng/µl (1µg/µl) using 50 mM Tris pH 7.5.

Transfection

Eukaryotic cell transfection was carried out using COS cells using Lipofectamine 2000 (Invitrogen) reagent in six well plates. Cells were plated 48h before transfection at cell densities of 1-2x10^5 cells/well in Dulbecos modification of Eagles medium (DMEM), 10% foetal calf serum without antibiotics,. Cells were viewed under a light microscope before transfection to verify that they were 90-95% confluent. For transfection, per well, 4µg of DNA was diluted in 50µl of Opti-MEM I medium (Invitrogen). In a separate tube, Lipofectamine 2000 was also diluted in Opti-MEM I reduced serum medium (10µl in 50µl). These dilution products were combined, incubated for 20 minutes and the 100ul resultant mix added drop wise to the COS cells. Cells were returned to the 37^{o}C incubator for a further 48-72 hrs. Following this, cells were harvested into 1ml of sterile PBS, centrifuged and the cell pellets were stored at -20^{o}C. Cell pellets were lysed using lysis buffer (50 mM Hepes pH 7.5, 150 mM NaCl, 1.5 mM $MgCl_2$, 1mM EGTA, 1% Triton X) and the cellular extracts were stored at -80^{o}C.

Quantifying the protein

The protein concentration in produced from COS cell lysates were quantified using a BioRad Dc protein assay kit, using a 96- well flat bottom plate and bovine serum albumin as a standard control. Samples were added neat and 1:5 diluted in PBS or lysis buffer, a standard curve was produced using serial dilutions of BSA, at 2, 1, 0.5, 0.25, 0.125, 0.063 and 0.031 mg/ml respectively. Readings were measured using a wavelength of 750 nm.

SDS-PAGE and Western Blots

SDS-PAGE and Western Blots were used to visualise proteins that were present in the transfected cell lysates. 12.5% polyacrylamide gels were made for the separation of the

proteins, samples were prepared using 5x SDS+DTT buffer, various volumes were loaded onto the gels and transferred onto a polyvinylidene fluoride (PVDF) membrane allowing for visualisation of the proteins. Blots were blocked with 5% milk powder in TBS-Tween (1%) for 1hr at room temperature or overnight at 4°C. After blocking the blots were probed with primary antibodies (see table). The secondary antibodies used were goat anti mouse and goat anti rabbit antibodies conjugated to horse radish peroxidise (1:20000) (Sigma) and proteins were visualised by enhanced chemiluminescence (ECL) substrate and autoradiography.

	Antibody	Dilution	Source
Amigo1-Flag	Mouse anti-Flag	1:1000	Sigma F3165 1MG
Amigo2-Flag	Mouse anti-Flag	1:1000	Sigma F3165 1MG
Amigo3-Flag	Mouse anti-Flag	1:1000	Sigma F3165 1MG
NgR	Mouse anti-NgR	1:500	R& D Systems MAB1208 500ug
$p75^{NTR}$	Rabbit anti-NGFR Mouse anti-NGFR	1:1000 1:1000	Promega G323A Millipore MAB5264
β actin	Mouse anti- actin	1:10000	Sigma A5441

Table 2.1. Antibodies used in western blots.

Stripping and re-probing the membrane

After the protein of choice had been detected on the membrane, the membrane was treated with mild stripping buffer (1.5% glycine, 0.1% SDS, 1% Tween-20 pH 2.2) then re-probed for actin to quantify protein loading. The buffer was added to the membrane for 3hrs after then washed twice in PBS, for 5mins each and twice in TBS-Tween, for 5mins each.

Deglycosylation

Deglycosylation was performed by adding 4µl of Glycoprotein denaturing buffer (NEB) to 20µl of cell lysates and 16µl of H_2O and boiling for 10 minutes. This was followed by taking 10µl of this reaction and adding 2µl of G7 reaction buffer, 2µl of NP40 and 1µl PNGase F followed by a 1hr incubation at 37^{o}C. These samples were treated in a similar manner to that of the glycosylated ones by adding the appropriate volume of 5x sample buffer +DTT and boiling for 5 minutes.

Co-Immunoprecipitation

Co-IPs were performed to determine the binding properties of the proteins of interest. DNA in various combinations was transfected into COS cells, 4µg of each construct were added to the cells which were left to grow for 48hours before being harvested and lysed. The cell lysates were then mixed with either anti-FLAG (M2 affinity beads, Sigma) or anti-HA (anti-HA affinity matrix, Roche) beads for 2hours, the beads were then washed with lysis buffer twice and finally sample buffer +DTT was added and the beads were boiled for 2minutes. Samples were stored at -80^{o}C and analysed by western blot.

3. Results

3.1 Cloning of NgR, p75 and Amigo 1-3.

NgR, $p75^{NTR}$ and Amigo 1, 2 and 3 products were produced by PCR. FLAG tags were incorporated into the Amigo 1, 2 and 3 constructs by removing the native 3' stop codons leading to fusion with the recipient plasmid (pAAV-IRES-hrGFP) 3x FLAG sequences, whilst NgR and p75 were left in their native forms. Primers incorporating EcoRI, BamHI or XhoI restriction sites were used for cloning and the products of PCR amplification were run on agarose gel electrophoresis for analysis and purification. Amigo1 contains EcoRI and XhoI restriction sites and the PCR product is 1476bp in size, Amigo 2 contains BamHI and XhoI restriction sites and the products are 1569bp in size (Figure 3.1). The native Amigo 3 cDNA sequence contains internal BamHI and EcoRI sites, precluding straightforward cloning. The internal BamHI site was therefore mutated by overlap extension PCR, a two step PCR process in which, in combination with external primers, overlapping internal mutagenic PCR primers are used to create two intermediate complimentary products. The two products are then fused using a subsequent PCR step to create a full length PCR product containing the desired mutant (in this case removing an internal BamHI site) (Fig 3.2.). NgR and $p75^{NTR}$ cDNA did not contain any internal restriction sites so straightforward PCR reactions were carried out as for Amigo 1 and Amigo 2.

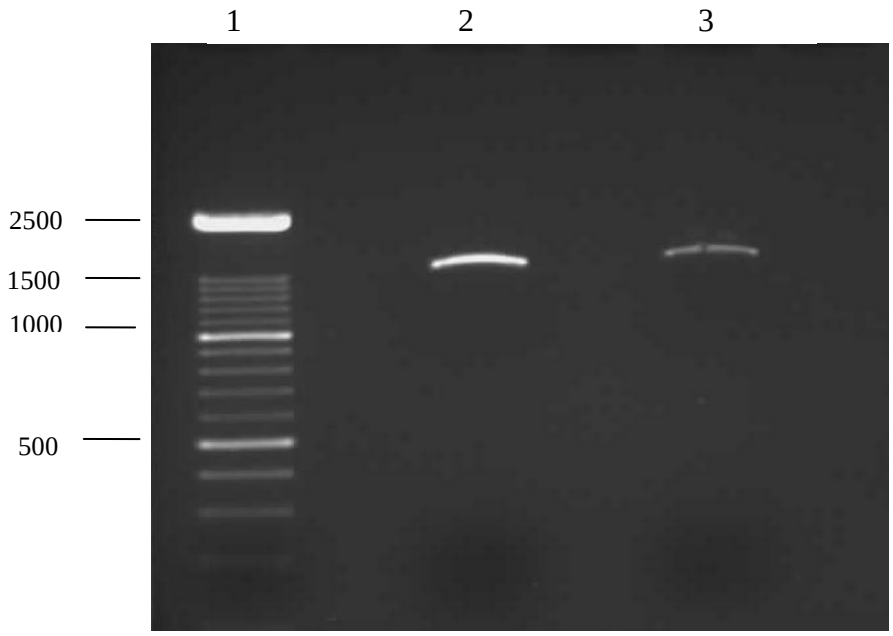

Figure 3.1. Gel electrophoresis of digested Amigo1 and Amigo2 inserts.

Lane 1 shows the 100bp DNA ladder (Roche), lane 2 contains digested Amigo1 at 1476bp and lane 3 contains digested Amigo2 at 1569bp.

PCR products were analysed by agarose gel electrophoresis along side a DNA ladder to determine if the reaction had worked and produced a product and that the product was of the correct size. Next, bands containing DNA of the correct sizes were excised from the agarose and the DNA was purified and digested for 2hours with either EcoRI and XhoI or BamHI and XhoI to produce sticky ends on the DNA insert. The digested products were analysed by agarose gel electrophoresis (Figures 3.1 and 3.3) followed by excision of the DNA bands and purification of the DNA ready for ligation.

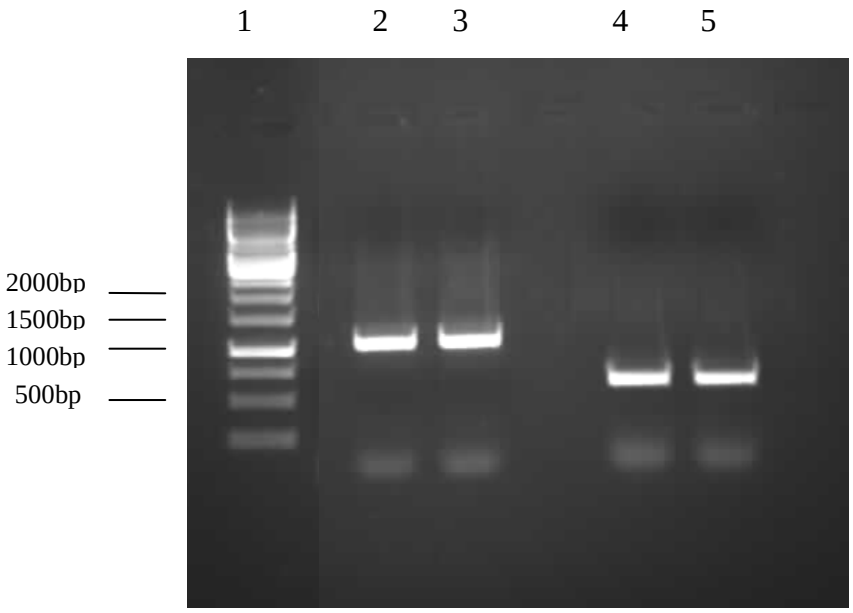

Figure 3.2. Products of overlap extension PCR.

Lane 1 shows the 1Kb DNA ladder (Fermentas). Lanes 2 and 3 and 4 and 5 show the products of the first step of the mutagenesis of Amigo 3, with the 5' product in lanes (2+3) and 3' product in lanes (4+5), with an overlapping region including the mutagenised BamHI site. The products were fused together via a subsequent PCR step to form a single full length Amigo 3 without the internal BamHI restriction site.

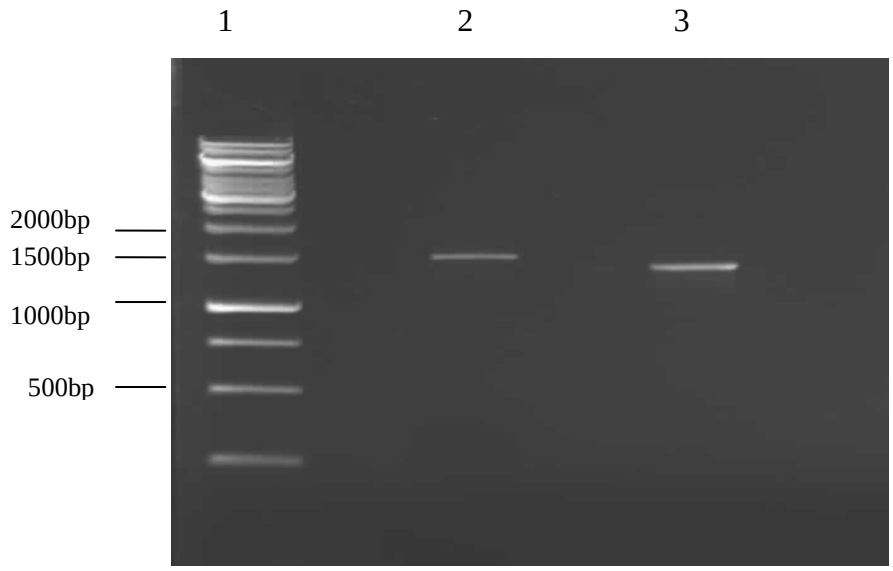

Figure 3.3. PCR amplification and digestion of NgR and p75^{NTR}.

Lane 1 shows the 1Kb DNA ladder (Fermentas) NgR and p75^{NTR} digestion products are shown in lanes 2 and 3 respectively.

The pAAV-IRES-hrGFP vectors were digested with the same combination of enzymes (BamHI/XhoI or EcoRI/XhoI), dephosphorylated for 30 minutes (Antarctic phosphatase, NEB) and gel purified. Cut plasmid and digested PCR products were ligated using T4 DNA ligase for between 1 hour and overnight. The ligation mixes were transformed into chemically competent E.coli cells (Top10 cells) by heat shock which were then plated onto LB/agar/ampicillin plates overnight. Typically, six single colonies were picked off each plate and grown overnight in 5ml LB media. Bacterial cultures were then mini prepped to extract the DNA from each. The mini prepped DNA was PCR screened, using the primers that were used to originally amplify the DNA, to see which of the clones contained the insert (Figure 3.4).

The presence of an insert was confirmed by DNA sequencing, initially using a β-globin primer which binds 5'of the DNA insertion site, enabling determination of the DNA sequence before the insert and then typically 800 bases of the insert itself. Positive clones were then sequenced using appropriate internal primers (Table 2. Appendix) and analysed using Sequencher software (figures 3.5 and 3.6), comparing the DNA sequence results to the known nucleotide sequences for that protein acquired from the NCBI nucleotide database. All constructs were sequenced along their full length to confirm they corresponded to the designed sequence and were free of mutations.

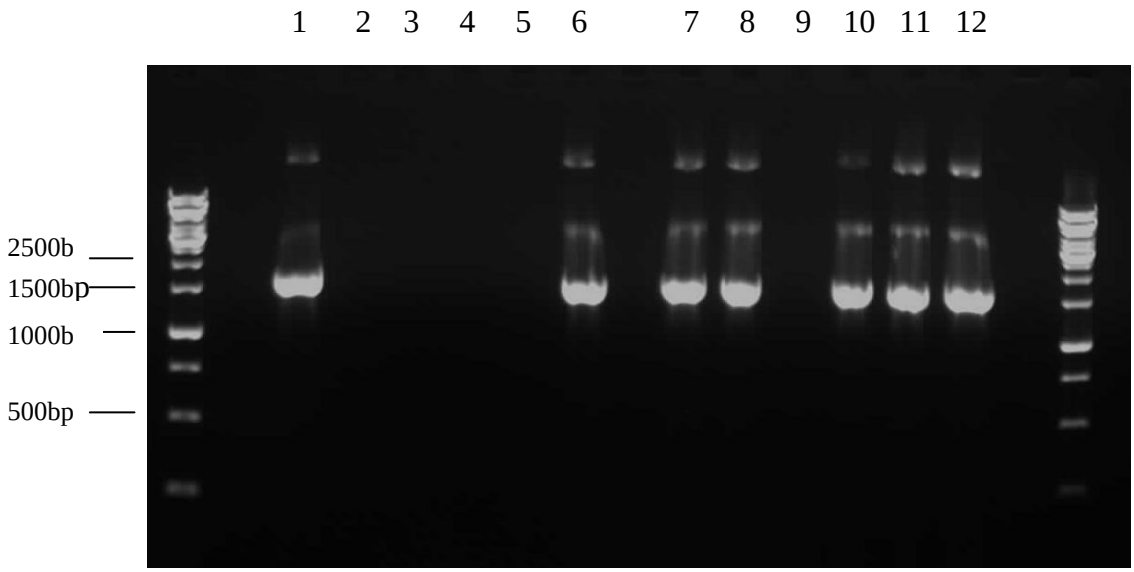

Figure 3.4 Analysis of clones containing DNA inserts.

Lanes 1-6 show Amigo 1 clones after PCR screening, clones 1 and 6 contain the DNA insert.

Lanes 7-12 show Amigo 2 clones after PCR screening, clones 7, 8, 10, 11, and 12 all contain the DNA insert.

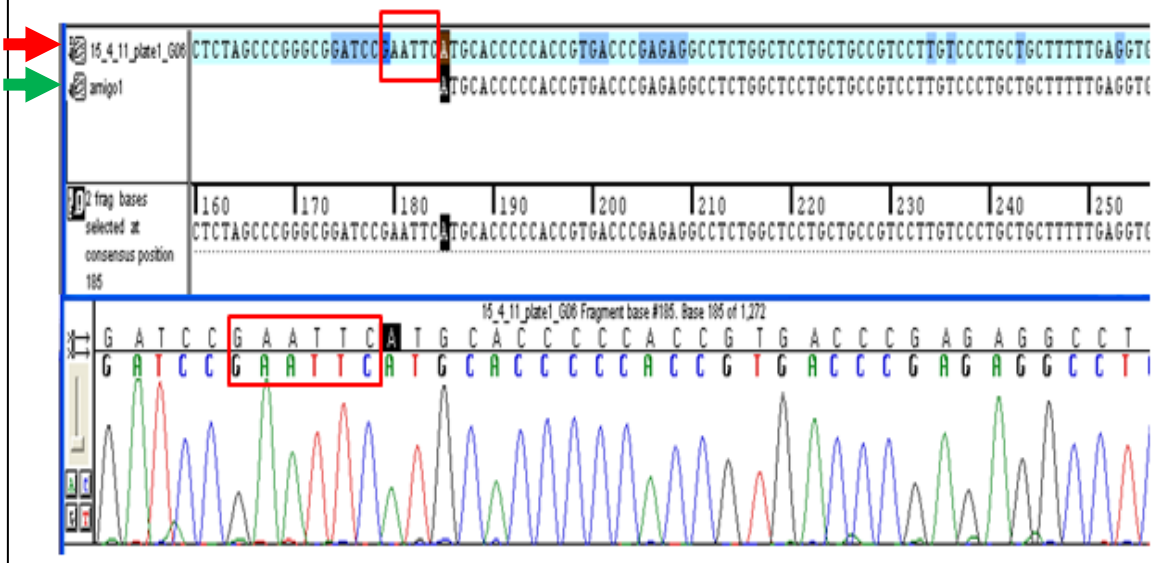

Figure 3.5. DNA sequencing results of 5' end of representative clone containing Amigo1.

DNA sequence results of an Amigo 1 clone using the β- globin primer (red arrow) compared to the known sequence for Amigo 1 (green arrow) as shown in Sequencher software. The EcoRI restriction site is boxed in red; this is followed by the Amigo 1 DNA insert. The chromatogram is shown below; each peak represents a different nucleotide with red being thymine (T), green representing adenine (A), black representing guanine (G) and blue representing cytosine (C).

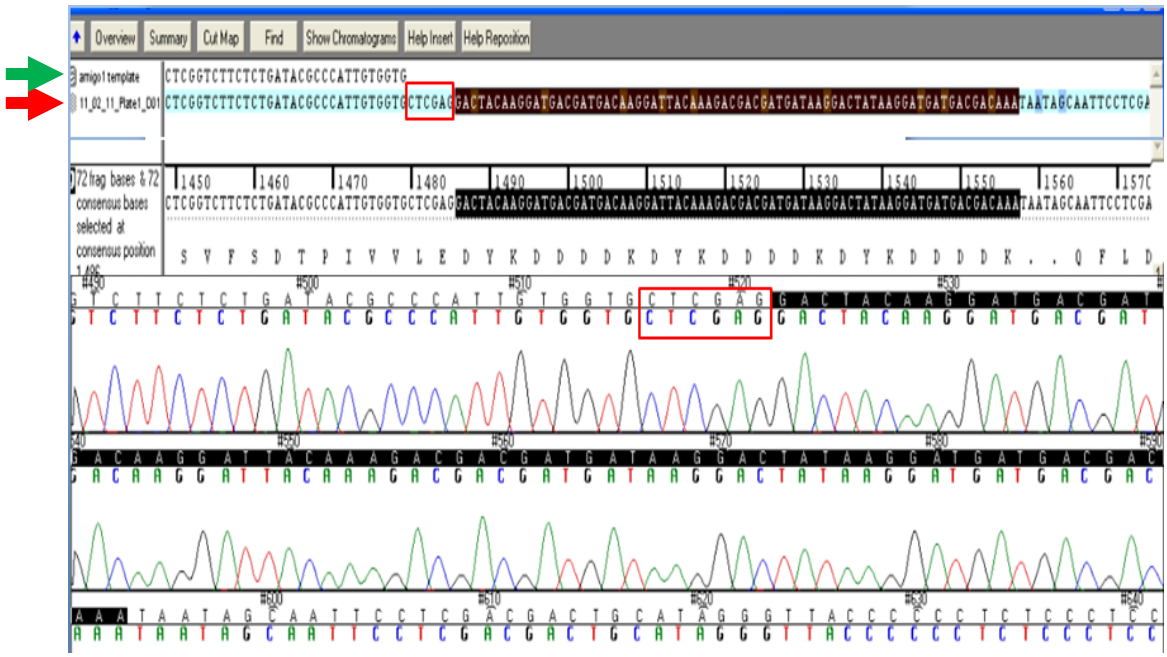

Figure 3.6. DNA sequencing results of 3' end of clone containing Amigo 1.

DNA sequence results of Amigo1 followed by 3 FLAG tags analysed in Sequencher software. The Amigo 1 clone DNA sequence (red arrow) is compared to the known Amigo1 sequence (green arrow). The XhoI restriction site is boxed in red on both the base sequence and the chromatogram, the FLAG tag sequence is shown by the white letters on a black background. The Chromatogram is shown for the Amigo1 clone; each peak represents a different nucleotide with red being thymine (T), green representing adenine (A), black representing guanine (G) and blue representing cytosine (C).

Colonies corresponding to analysed NgR, p75, Amigo1, Amigo2 and Amigo3 clones were expanded in 100ml cultures to allow larger scale preparation of the DNA using a midi prep kit. The concentration of DNA extracted was measured by nanodrop and then all DNA was diluted to a concentration of 1000ng/ul (1ug/ul) with elution buffer for further use.

3.2. Analysis of Amigo, NgR and p75^{NTR} expression/ Expression of Amigo, NgR and p75^{NTR} constructs in mammalian cells.

Amigo 1, 2 and 3 (-FLAG) were transfected into COS cells, using the Lipofectamine 2000 (Invitrogen) method. Following transfection, COS cells were grown for between 48 and 72 hours at 37^{o}C, following which they were harvested and lysed with lysis buffer. To determine the concentration of protein in the cellular lysates a protein assay was performed, where the cell lysates were compared to a BSA at known concentrations, starting at 2mg/ml, followed by seven doubling dilutions. Cell lysates were added neat and diluted 1:5 to ensure OD readings over a linear range of concentrations, with all samples run in duplicate. The plate was read in an ELISA plate reader and the average OD reading of the duplicates was used to determine protein concentrations.

a)

2	2	Neat	Neat	Neat	Neat	Neat	Neat
1	1	1:5	1:5	1:5	1:5	1:5	1:5
0.5	0.5						
0.25	0.25						
0.125	0.125						
0.063	0.063						
0.031	0.031						
Blank	Blank						

b)

0.297	0.321	0.413	0.337	0.322	0.321	0.304	0.296
0.122	0.200	0.113	0.145	0.125	0.123	0.155	0.119
0.136	0.132						
0.099	0.094						
0.076	0.072						
0.063	0.061						
0.057	0.055						
0.050	0.052						

Figure 3.7. Results from BioRad Dc Protein Assay.

a) Layout of plate; BSA was added in duplicate to the dark blue columns in the concentrations (mg/ml) indicated, samples were added in duplicate to the pale blue wells neat and diluted 1:5.

b) OD readings from plate reader; the readings for the proteins were compared to the readings for the BSA control.

The protein assay indicated that, broadly speaking, the lysate concentrations were roughly equivalent. As the subsequent analyses were semiquantitative only and would use western blotting for actin as a loading control, no dilutions were made for the protein lysates

.

Following the protein assay, proteins were analysed by Western Blot to determine their relative sizes. Amigo 1,2 and 3 cell lysates were prepared using Sample buffer + DTT and run on 12.5% SDS gels, with 10 µl and 2 µl samples of each run in parallel. Proteins were then transferred onto nitrocellulose membrane, the membrane was then blocked in 5% milk, washed, and probed with a mouse anti-FLAG antibody then with a goat anti mouse 2^{o} antibody conjugated to HRP before being developed by ECL (Figure 3.8).

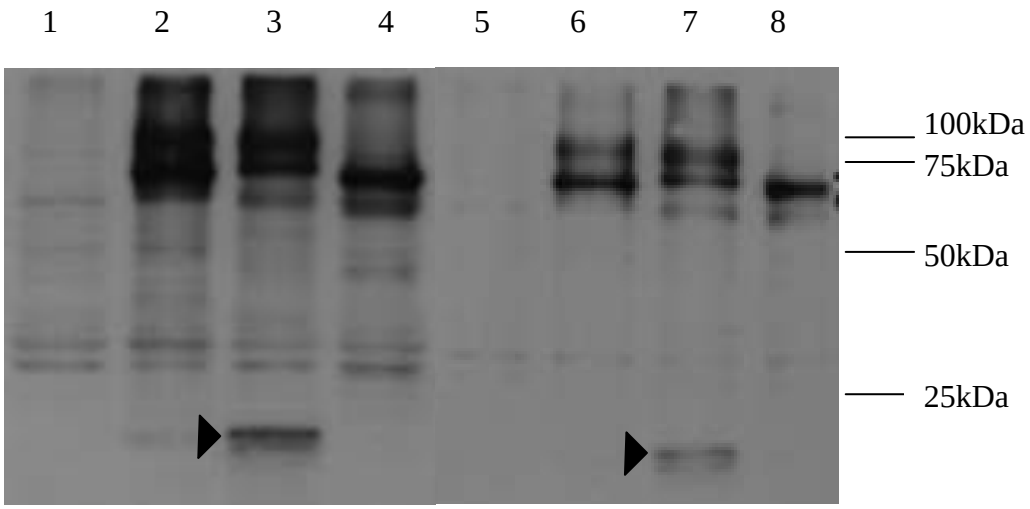

Figure 3.8. Western Blot analysis of the Amigo 1, 2 and 3 proteins.

Lanes 1 and 5 show COS cell lysates, 2 and 6 show Amigo1 cell lysates, 3 and 7 show Amigo2 cell lysates and lanes 4 and 8 show Amigo3 cell lysates. Lanes 1-4 were loaded with 10µl of cellular lysates and lanes 5-8 were loaded with 2µl of cellular lysates. Lanes 3 and 7 contain a small molecular weight species at around 20 kDa, these are indicated by the arrow heads.

The Western Blot showed us that the Amigo proteins were successfully expressed in COS cells, the Amigo proteins are shown to be roughly 75kDa in size, with Amigo 1 and Amigo 2 running as doublets. In addition, the lanes corresponding to the Amigo 2 protein lysate consistently displayed a small band at 20 kDa, potentially indicating cleavage of full length Amigo 2 to produce a free or membrane bound intracellular domain. The observed protein doublets could result from differential gylcosylation, so the protein lysates were treated with PNGase (also known as N-Glycosidase F) to hydrolyse and remove N-glycan chains. The enzyme cleaves between the innermost GlcNAc and asparagine residues of high mannose, hybrid, and complex oligosaccharides from N-linked glycoproteins to reveal monomeric forms of proteins. After deglycosylation the Amigo proteins were analysed as before by Western Blot alongside the original glycosylated proteins (Figure 3.8), this showed that the double bands were due to differential glycosylation as they became singular after enzyme treatment. The size of the proteins changed due to this and the more realistic estimate of the size of the products now approximates to 55 kDa.

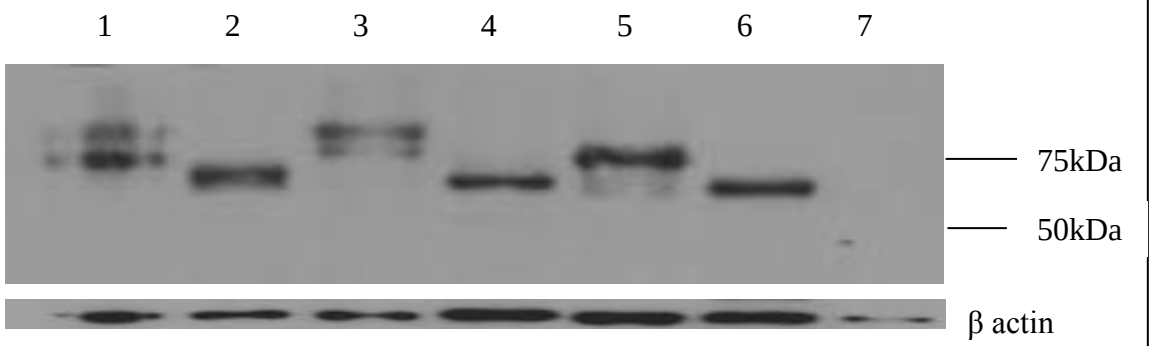

Figure 3.9. Deglycosylation of Amigo proteins.

Lanes 1, 3 and 5 contain Amigo 1, Amigo 2 and Amigo 3 cell lysates respectively. Lanes 2, 4 and 6 contain the Amigo 1, Amigo 2 and Amigo 3 cell lysates after deglycosylation respectively. Lane 7 contains the COS cell lysate. 10µl of sample was added to each lane.

COS cells were also transfected with NgR and $p75^{NTR}$ constructs and again left to grow for 48-72 hours. Lysates were analysed by western blots using anti- NgR and anti- $p75^{NTR}$ antibodies. Membranes were stripped using stripping buffer and then re-blocked and re-probed for actin.

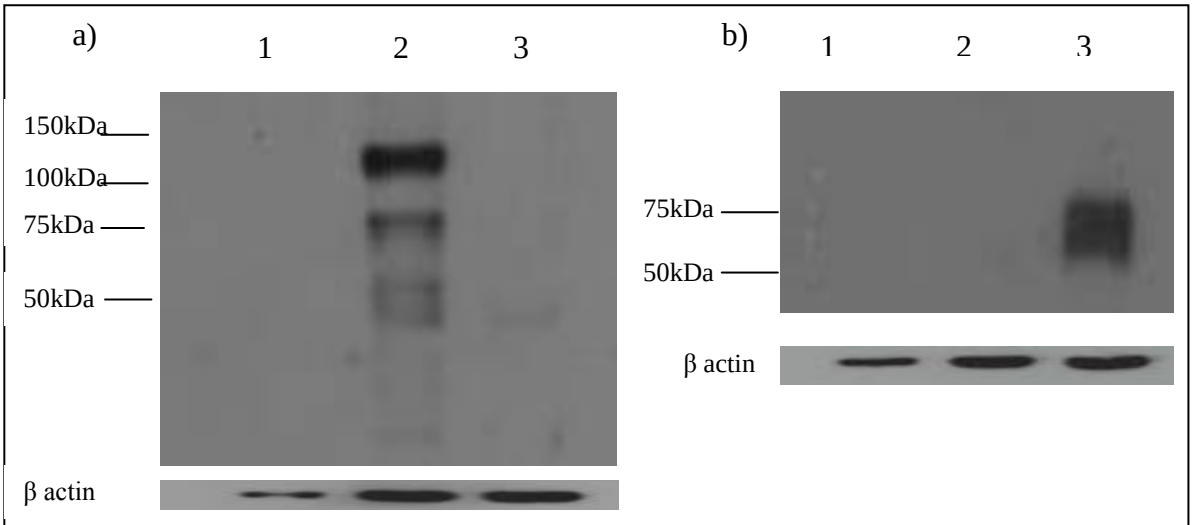

Figure 3.10. NgR and $p75^{NTR}$ cell lysates probed with anti-NgR or anti-$p75^{NTR}$ antibodies.

a) Western blot using an antibody against NgR. Lane 1 contains COS cell lysates, lane 2 contains NgR cell lysates and lane 3 contains $p75^{NTR}$ cell lysates.

b) Western blot using an antibody against $p75^{NTR}$. Lane 1 contains COS cell lysates, lane 2 contains NgR cell lysates and lane 3 contains $p75^{NTR}$ cell lysates.

2ul of each sample was added to the wells.

These western blots showed that the transfections with NgR and $p75^{NTR}$ were successful and the proteins were present in the cellular lysates, without cross-reactivity between NgR $p75^{NTR}$ antibodies.

Once individual protein expression was established next we wanted to investigate how the different molecules interact when expressed together. Co-IP experiments were performed to see if any of the Amigos would bind to NgR or $p75^{NTR}$. Relevant combinations of plasmids were transfected into COS cells, which were grown for 48hrs then lysed as before. Anti FLAG beads were added to cellular lysates and mixed, washed and run by SDS-PAGE as before. The blots were then probed with anti-NgR or anti-$p75^{NTR}$ antibodies.

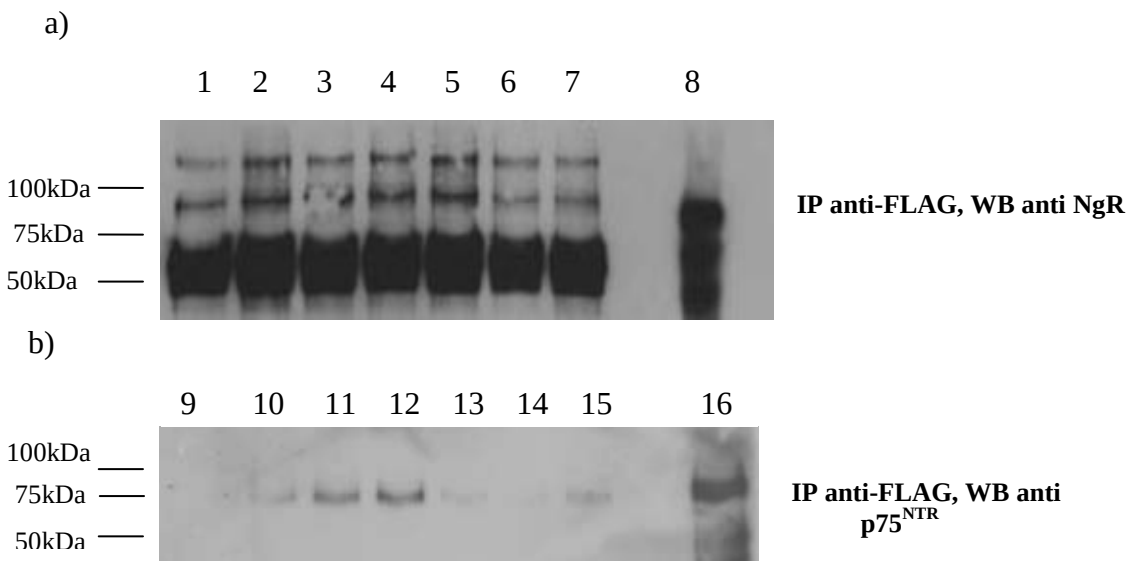

Figure 3.11. Co-IP experiments of the Amigo proteins with NgR and $p75^{NTR}$.

a) Lane 1 contains COS cell lysate, lanes 2, 3, and 4 contain NgR + Amigo1, Amigo 2 and Amigo 3 co-IPs respectively. Lanes 5, 6, and 7 contain NgR+ $p75^{NTR}$ + Amigo1, Amigo2 and Amigo3 co-IPs respectively (as do lanes 13, 14 and 15). Lane 8 contains NgR cell lysate.

b) Lane 9 contains COS cell lysate, lanes 10, 11 and 12 contain $p75^{NTR}$ + Amigo1, Amigo2 and Amigo3 co-IPs respectively lane 16 contains $p75^{NTR}$ cell lysates.

Immunoprecipitating with anti FLAG blotting with anti- $p75^{NTR}$ produced bands corresponding to the size of p75NTR, suggesting co-immunoprecipitation of $p75^{NTR}$ with Amigo 1, 2 and 3 (lanes 10, 11, 12). The band intensity was reduced significantly in lysates with Amigo 1-3 and both NgR and p75 lanes (13, 14, 15). These results could indicate differential binding of individual Amigo proteins to $p75^{NTR}$, which could be further influenced by the presence of NgR. Alternatively, particularly as the method is only semiquantitative at best, the findings could be a consequence of interference of individual plasmid constructs with one another during the transfection process (for example, the addition of NgR plasmid to the transfection mix could reduce the efficiency of $p75^{NTR}$ plasmid transfection).

Results from the anti NgR probing were more difficult to interpret, with numerous bands present in all wells (including non transfected COS lysates). The most prominent bands were 55kDa in size, suggesting that these bands were potentially contaminating immunoglobulin heavy chains from the beads – which would have been detected by the secondary antibody (goat anti mouse) in the western blot stage.

The co-IP experiment had so far been looking at what binds to the Amigo proteins by using anti-FLAG beads, but the NgR and $p75^{NTR}$ constructs made were not tagged so it was not possible to isolate these proteins and see what binds to them. It was decided to tag NgR and $p75^{NTR}$ with a HA tag so that co-IP experiments could be performed using anti-HA beads. Overlap extension PCR was performed on the NgR and $p75^{NTR}$ DNA constructs to add the HA tag then the co-IP experiments were performed by transfecting the COS cells as before with different combinations of the DNA of interest. The beads were anti-HA beads which were mixed with the cell lysates to bind to and isolate the proteins with

HA tags on and consequently those proteins that were in turn bound to them. The beads and their bound proteins were boiled with Sample buffer +DTT and loaded into a 12.5% protein gel, the blots were then probed with anti-FLAG antibodies which would reveal of any of the Amigo proteins bound to the NgR or $p75^{NTR}$ protein.

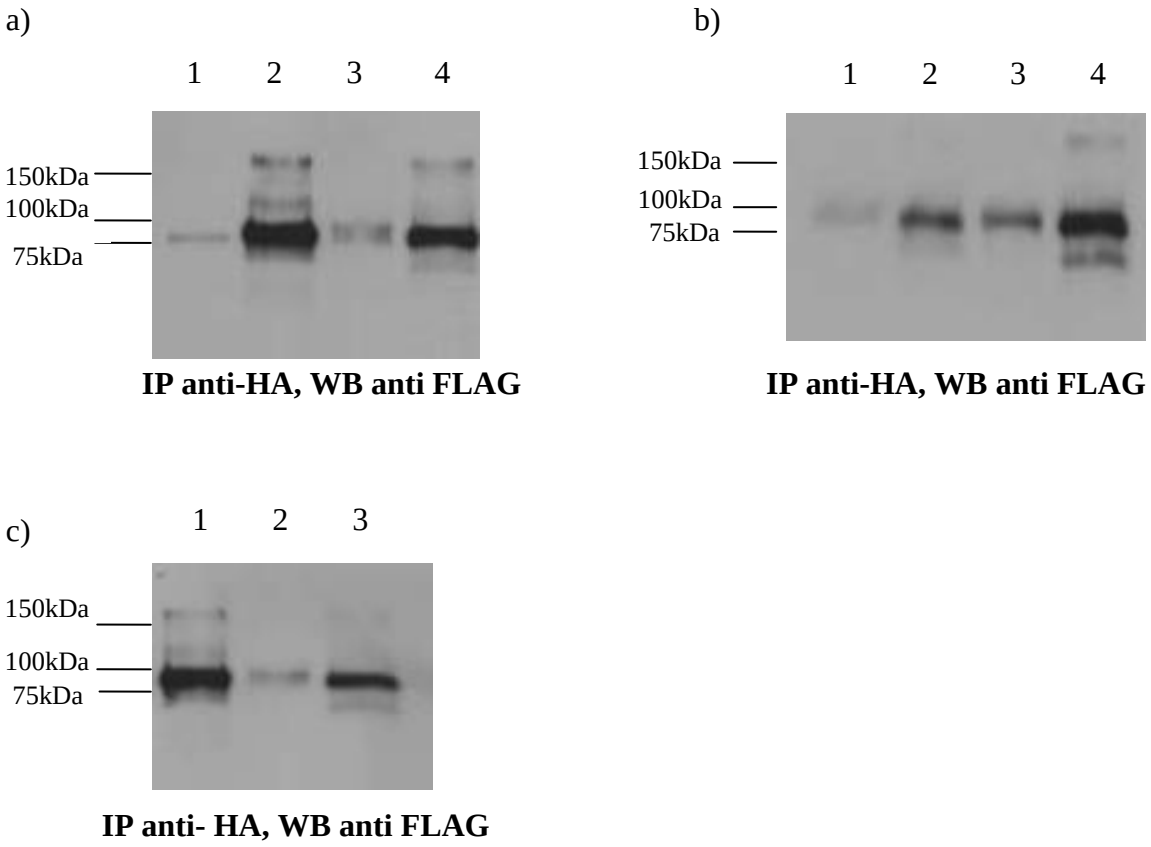

Figure 3.12. Co-IP experiments with HA tagged NgR and $p75^{NTR}$ and the Amigo proteins.

- a) Lane 1 contains the NgR cell lysate, lanes 2, 3 and 4 show NgR-HA immunoprecipitated with Amigos1, 2 and 3 respectively.
- b) Lane 1 contains the $p75^{NTR}$ cell lysate, lanes 2, 3 and 4 show $P75^{NTR}$-HA immunoprecipitated with Amigos1, 2 and 3 respectively.
- c) Lanes 1, 2 and 3 show NgR+$p75^{NTR}$ and Amigos1, 2 and 3 respectively.

To make to most of the different ways in which a co-IP could be carried out we decided to clone various versions of the Amigo proteins, i.e. we made wild type versions, HA tagged versions and double tagged HA/FLAG versions to go along with the FLAG tagged Amigo proteins already made.

4. Discussion

Human Amigo 1 and Amigo 2 were cloned successfully into mammalian expression vectors, as was human Amigo 3, which was cloned with its internal BamHI restriction site removed by mutagenesis. All three of the Amigo constructs had their stop codons removed, resulting in the incorporation of triple FLAG tag sequences to their 3' ends (from the expression vector), to enable identification and isolation. DNA sequencing throughout the length of the respective genes revealed that no mutations had occurred during the cloning processes. Amigo 1, Amigo 2 and Amigo 3 plasmid DNA were subsequently transfected into COS cells. Human NgR and $p75^{NTR}$ were also cloned successfully, using standard approaches, as no internal restriction sites had to be removed and no tags were added to the 3' end of the DNA. Similarly, no mutations were found in the cloned DNA of NgR or $p75^{NTR}$ after sequencing. DNA was transfected into COS cells and cellular lysates were analysed by western blot to determine the transfection efficiency and levels and patterns of protein expression. Western blots (figure 3.8) revealed high levels of expression for Amigo 1, Amigo 2 and Amigo 3 which are around 70 kDa in size. Of interest, a significant lower molecular band was consistently identified in the Amigo 2 cell lysate, at around 20 kDa, suggesting the protein is potentially cleaved. The specific cleavage site is the subject of speculation, but would be likely to be extracellular but membrane proximal, to incorporate the cytoplasmic domain which contains the FLAG sequences essential for detection. This assumption is based on the observation that the transmembrane region is 21 amino acids (residues 399-419) and intracellular domain 103 amino acids long (amino acids 420-522) respectively. The calculated size for these two regions is 2257 and 10831 daltons, to which the FLAG tag region would be added.

In this western blot the Amigo protein bands were shown as doublets which made an accurate evaluation of molecular masses difficult. The pattern could be the result of impurities or breakdown products, but a more likely cause for the doublet appearance was of variable glycosylation. It is predicted that Amigo 1 has N-linked gylcosylation sites on 5 amino acids (residues; 7, 264, 315, 349 and 360), Amigo 2 has N-linked gylcosylation sites on 8 amino acids (residues; 58, 104, 281, 288,345, 373, 381 and 384) and Amigo 3 has N-linked gylcosylation sites on 5 amino acids (residues; 107, 272, 301, 362, 368) (UniProtKB protein database). This possibility was therefore analysed by deglycosylating the relevant cell lysates using PNGase, an enzyme which removes almost all N-linked oligosaccharides from glycoproteins. The deglycosylated protein lysates were analysed alongside their glycosylated counterparts (figure 3.9) by Western blot. Bands produced by the deglycosylated proteins now migrated as singlets, shifting their apparent molecular weight to 60 kDa.

In contrast, Western blots performed on NgR and $p75^{NTR}$ cell lysates (figure 3.10) revealed only single major bands at 120 kDa (NgR) and 75 kDa ($p75^{NTR}$) showing no clear differential glycosylation. The blot did however show a number of potential breakdown products in the NgR lysate, although this suggestion will require further analysis. This phenomenon has been previously described [36], in which an NgR construct transfected into CHO cells produced NgR species migrating at 64 kDa and 48 kDa, speculated to be a C-terminally truncated NgR fragment. In addition, the blotting also suggested that there was no cross reactivity between the NgR and $p75^{NTR}$ antibodies.

Following preliminary experiments where expression of the proteins alone was analysed, co-immunoprecipitation experiments were performed to determine the binding properties

of those proteins to one another. COS cells were transfected with Amigo 1, 2 or 3 DNA plus NgR and/or $p75^{NTR}$ DNA, allowed to grow for 48-72hrs and lysed. Initially anti-FLAG beads were used and were added to the COS cell lysates allowing the Amigo proteins to bind via their FLAG tag regions. The beads were washed and analysed by western blot using antibodies directed to either NgR or $p75^{NTR}$ to determine if either of these proteins had bound to the any of the Amigo proteins. The blots (Figure 3.11) showed that the anti NgR antibody was poor because the antibody bound in all cases even in the COS cell lysate (which contained neither Amigo nor NgR). Probing for $p75^{NTR}$ gave more promising results, revealing that $p75^{NTR}$ binds to Amigos 1 and 3 with and without NgR present and binds Amigo 2 in the absence of NgR.

Because of the promising results obtained from the first set of co-IP experiments, NgR and $p75^{NTR}$ were cloned with the addition of N-terminal HA tags. Co-IP experiments were then performed using anti-HA beads to bind to either NgR or $p75^{NTR}$ in the COS cell lysate, the beads were analysed by western blot and probed using anti FLAG antibody to see if any of the Amigo proteins had bound. The western blot (figure 3.12) revealed a large amount of binding between NgR and Amigos 1 and 3 with and without $p75^{NTR}$ present, and also showed that $p75^{NTR}$ binds to Amigos 1 and 3 with and without NgR present. There is a small amount of binding between Amigo 2 and NgR and $p75^{NTR}$ alone and when NgR and $p75^{NTR}$ are expressed together which corresponds to the idea that Amigo2 binding is reduced due to the cleavage of an important region.

Future work

The experiments presented above need further replication, with investigation of the binding properties using a range of alternative biochemical and biophysical approaches. Some of these require the use of detergent free soluble proteins (therefore lacking their transmembrane regions). The proteins will therefore need to be expressed as protein ectodomains (best achieved using our established S2 drosophila system), preferably with structural variants to include the LRR region of each of Amigo protein, as well as the LRR regions plus the Ig region of the protein. Following successful expression, these proteins would be attached to a BiaCore chip and recombinant NgR and $p75^{NTR}$ proteins would be flowed over the chip to test for binding. As an alternative, the NgR and $p75^{NTR}$ proteins could be bonded with the chip and the Amigo ectodomains can be flowed over. Also, it would be useful to determine the structure of the expressed ectodomains of the Amigo proteins and X ray crystallography would be a good method to use for this.

It will be important to confirm that the proteins are expressed at the cell surface in native form. There are several experimental approaches that could be used, the most straightforward would consist of biotinylation of the cell surface of transfected cells (using a membrane impermeant form of biotin), followed by precipitation of biotinylated proteins with streptavadin-agarose and subsequent western blotting for proteins of interest. Alternatively, high resolution microscopy (confocal for example) could also be used to localise transfected proteins.

Another area to continue with would be the cloning of the DNA for all the proteins of interest in their native forms as well as with different tags on, i.e. for each protein there would be: wild type (WT), (amino-terminal) HA tagged, (carboxy-terminal) FLAG tagged and HA+FLAG tagged combinations, this will enable us to fully characterise the

respective binding and potential cleavage properties of these proteins, as suggested by the Western blotting patterns of Amigo 2.

Lingo is the best characterised component of the NgR/p75 complex and it would be desirable to repeat the co-immunoprecipitation experiments, using this protein as a positive control and potentially make semiquantitive assessments of comparative binding properties, including any heterophilic association with Amigo family members. Alongside this, similar experiments should be performed using TROY; as this protein is thought to substitute for $p75^{NTR}$ and is more widely expressed in the CNS and may have a more important function.

MRes Research Project 2

Adhesive Interactions of Mesenchymal Stem Cells with Platelets and P-selectin

THE UNIVERSITY OF BIRMINGHAM

Abstract

Mesenchymal stem cells (MSCs) are non haematopoietic cells capable of differentiating into adipocytes, chondrocytes and osteoblasts they are positive for CD105, CD90 and CD73 and negative for CD34 and CD45 amongst others. MSCs are not immunogenic and do not stimulate alloreactivity and this characteristic along with their ability to differentiate into such a range of cell types make them attractive for use in regenerative therapies by systemic infusion of ex vivo expanded cells. It s not known how MSCs are recruited from the circulation, however they may employ mechanisms similar to those used by leukocytes and haematopoietic stem cells when they are transported from the circulation such as the employment of selectins and via the aid of platelets. We therefore wanted to determine if MSCs can bind to collagen or P selectin coated microslides under flow conditions and in parallel observe if platelets as a whole can bind to MSCs in a variety of conditions by staining MSC and blood samples with CD105 (MSC marker) and CD42b (platelet marker) and use flow cytometry to looking at the effects of anticoagulant, time and platelet activation. The results demonstrated that MSCs do not bind to collagen or P selectin under flow conditions and demonstrated that a small proportion of platelets can bind to MSCs under appropriate conditions. Further, the binding experiments revealed that platelet activation reduced the level of binding between MSCs and platelets.

Acknowledgements

I would like to thank Professor Gerard Nash for his help and guidance throughout this project. I would also like to thank the members of the Nash lab for all of their help.

5. Introduction

Mesenchymal stem cells (MSCs) have potential to be used therapeutically due to their capability to differentiate and regenerate tissue and their immunomodulatory effects. However, little is known about the mechanisms by which they are recruited from the circulation to their target tissues if infused. In order to gain more insight into the mode of action of MSCs this report will look at the adhesive characteristics of MSCs that might aid in their recruitment, in comparison to the previously described methods employed by leukocytes and haematopoietic stem cells.

5.1. Types of stem cell

Stem cells are progenitor cells that have the ability for unlimited self renewal, maintaining, at the same time, the ability to differentiate into mature lineages [37], with each daughter cell having a more restricted differentiation potential and more specific phenotypic characteristics [38] . The most naïve stem cells are totipotent stem cells which can differentiate into embryonic as well as extraembryonic cells. Following these are pluripotent stem cells also known as embryonic stem cells (ESC) which are derived from the inner cell mass of the blastocyst. These cells can differentiate into all the cells of the three germ cell layers: the ectoderm, endoderm and mesoderm. It is this pluripotency that differentiates embryonic stem cells from adult stem cells which are more restricted multipotent cells capable of differentiating into a limited number of cell types. These adult stem cells, also known as somatic stem cells, are life long cells that exist to replenish cells as they die, either by normal wear and tear or by injury [39] and although they are classed as multipotent they retain some of the features of their pluripotent progenitors such as their ability to endlessly self renew. Haematopoietic, neural and mesenchymal are all types of

multipotent adult stem cells. In some animals stem cells can sometimes be identified quite precisely by their morphology and location [40] but in humans, stem cells are defined by their function, i.e. what cells they become. Haematopoietic stem cells (HSCs) are easily identifiable as differentiating into cells of myeloid lineage such as eosinophils, macrophages and neutrophils, and cells of lymphoid lineage such as NK cells, T cells and B cells. HSCs are stored in the bone marrow at a frequency of 1: 10000 to 1:100000 total blood cells [41]. Neural stem cells differentiate into neurons and glia, and mesenchymal stem cells differentiate into a variety of cells including osteocytes, adipocytes and chondrocytes.

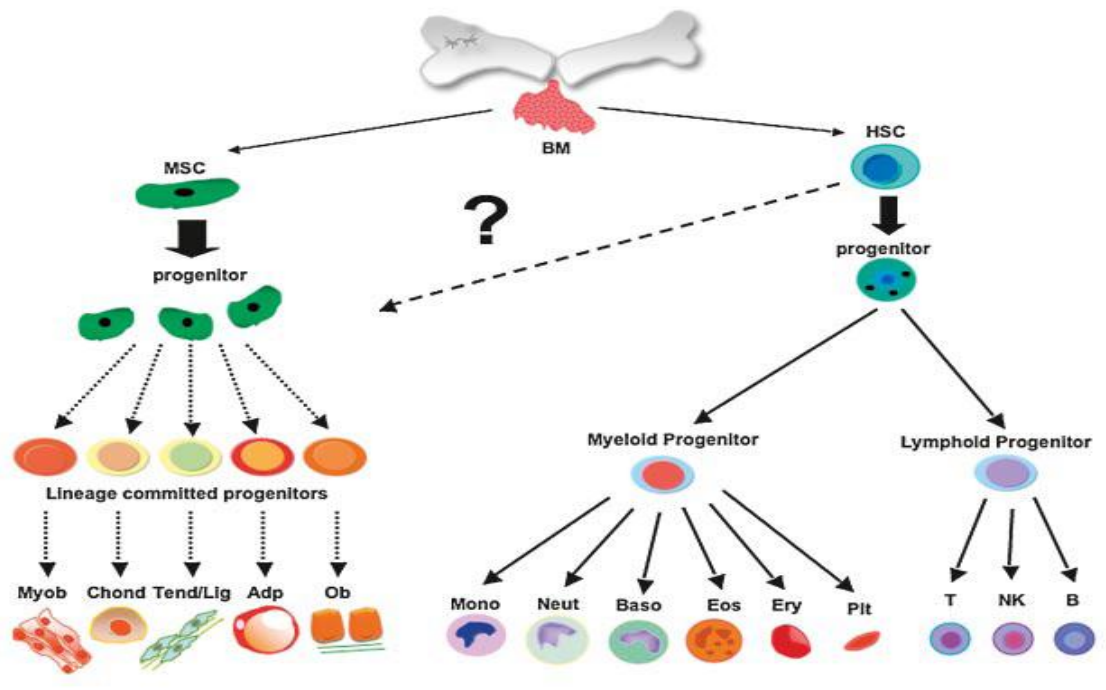

Figure 5.1. Diagrammatic representation of the differentiation of stem cells derived from bone marrow.

HSCs derived from the bone marrow differentiate into cells of myeloid (e.g. monocytes and neutrophils) and lymphoid (e.g. T and b cells) lineage. MSCs derived from the bone marrow differentiate into a number of cell types including chondrocytes, adipocytes and osteoblasts. [40].

5.2. Mesenchymal Stem Cells

Mesenchymal stem cells are non haematopoietic cells capable of differentiating into adipocytes, chondrocytes and osteoblasts and contribute to the renewal of adipose tissue, cartilage, bone, muscle, myocardium and marrow stroma [42], illustrating their diversity and meaning that MSCs are attractive for use in stem cell therapies. MSCs are so called because of their ability to differentiate into mesenchymal type cells, but it has been suggested many times that this may not be the most appropriate name to describe these cells as they differentiate into cells of both mesodermal and non mesodermal lineages i.e. ectodermal and endodermal lineages, and are therefore characterised as multipotent. Because of this, mesenchymal stem cells are often also referred to as; fibroblast colony forming units (CFU-Fs), bone marrow stromal cells [43], multipotent stromal cells or mesenchymal progenitor cells.

Phenotypically, MSCs have been difficult to classify because they display a great heterogeneity and many of the characteristic markers used to identify these cells are also exhibited by other cells. But despite the fact that no unique markers for MSCs have been found yet, their cell surface antigen expression profile has been well characterised; it has been shown that MSCs, unlike HSCs, are $CD34^-$ and $CD45^-$. MSCs have however been shown to be positive for; CD10, CD13, CD90, CD105, CD109 and CD164 among others [44] and are also HLA class 1 positive [45]. With these findings in mind the Mesenchymal and Tissue Stem Cell Committee of the International Society for Cellular Therapy came up with a set of guidelines to define MSCs [46], these were: cells must first be positive for CD73, CD90 and CD105, second they must be negative for HSC marker CD34, and leukocyte marker CD45 as well as CD14 or CD11b, and CD79a or CD19, and HLA-DR [47]. To term a cell an MSC it must also be plastic adherent and must be able to

differentiate into adipocytes, osteoblasts and chondroblasts under specific *in vitro* differentiating conditions [48]. It is worth noting that the above definitions are based on cells cultured *in vitro* and little is known about the phenotypic characteristics *in vivo*, their anatomical localisation or their contribution to organogenesis [49]. *In vivo* characterisation of MSCs would be extremely promising in providing therapeutic manipulations of these stem cells.

MSCs are most prevalent in the bone marrow where their frequency has been estimated to be around 1 in every 3.4 x 10^4 cells [50]. Within the bone marrow MSCs are an important member of the HSC niche and help to generate the microenvironment necessary for the maintenance, proliferation and differentiation of HSCs [50]. The number, frequency and differentiation capacity of MSCs decreases with age within the bone marrow [51]. Whilst the bone marrow is the most highly populated location of MSCs, they have been found in most tissues, although the exact localizations of MSCs *in vivo* are still improperly understood. MSCs were classified according to the characteristics displayed by cultured cells. However, when MSCs are cultured *in vitro* they may display markers that may not be displayed on the cell *in vivo* due to not being surrounded by all the extrinsic factors supplied by the physiological stem cell niche, and so it becomes difficult to establish the true identity of MSCs in their natural environments. Various methods have been used to try and establish which tissues MSCs reside in, including using stem cell markers known to be expressed on cells *in vitro* to look for the cells *in vivo* or infusing marked cultured stem cells *in vivo* and following their distribution[52]. Studies have found MSCs in adipose tissue [53], amniotic fluid [54] and dental pulp [55]. These findings are in agreement with results obtained by Young, H et al [56] which led them to conclude that progenitor and pluripotent stem cells are located in all organs having a connective tissue

compartment. Another method used to determine the location of MSCs is to isolate tissues and evaluate each of them for the presence of MSCs. By simultaneously analysing different tissues and organs for their MSC contents, Da Silva Meirelles et al [52] found MSCs in the brain, spleen, kidney, lung, liver, bone marrow, muscle, thymus and pancreas and found that they each displayed similar morphology. The animals used in this study were perfused before the organs were removed, the blood was analysed for the presence of MSCs but none could be cultured indicating that MSCs are absent from the blood under normal physiological conditions. But whilst many studies have been unable to locate MSCs in the normal peripheral circulation [57], some studies have been successful; Zvaifler et al. [58] found cells that expressed MSC marker CD105 and were capable of differentiating into adipocytes or osteoblasts under appropriate conditions in the peripheral blood. Also, Mansilla et al [59] found not only MSCs in the blood but also found that their numbers were increased in samples taken from patients who had suffered acute burns, indicating that they enter the circulation in response to injury.

In addition to being able to differentiate into various cell types, MSCs have been shown to provide cytokine and growth factor support for expansion of haematopoietic and embryonic stem cells [60]. MSCs express a range of cytokines including G-CSF, SCF, LIF, M-CSF, IL-6 and IL-11 [61] and the levels of expression of these cytokines is partly controlled by the environment around the stem cell niche and the actions of inflammatory stimuli (e.g. TNFα) acting on the MSCs themselves.

MSCs not only provide cytokine support the are also known to have immunomodulatory effects, MSCs are known to suppress the activation and proliferation of CD4+ and CD8+ lymphocytes in vitro [62], they have also been shown also to affect the function of antigen

presenting cells; MSCs reduce the expansion of dendritic cells (DC) and natural killer (NK) cells [63]. Those DCs that do form have a reduced potential, this was shown by Xiao-Xia Jiang et al [64] who found that DCs isolated from co-cultures with MSCs had a reduced potential to activate allogenic T cells. Conversely, MSCs cause an increase in the number of CD4+ CD25+ regulatory T cells [65]. Plumas J et al. [66] found that MSCs inhibited the proliferation of T cells in the presence of a number of different stimuli, and further discovered their mode of action was inducing the apoptosis of activated T cells whilst having no effect on resting T cells. MSCs have also been shown to significantly reduce the expression of activation markers CD25, CD38, and CD69 on the surface of stimulated lymphocytes [62] and human MSCs have been shown exert their suppressive effects even when MSCs and lymphocytes are separated by a permeable membrane [67] suggesting that soluble factors may be involved. Further, soluble factors secreted by the MSCs have suppressive effects but the culture medium of MSCs has been shown to have no effect on lymphocytes unless the MSCs were co cultured with the lymphocytes. This indicates that the MSCs do not normally express the suppressive factors and therefore suggests that there is some kind of cross talk between the cells which causes the MSCs to become activated and secrete the soluble suppressants [68].

MSCs are not immunogenic and do not stimulate alloreactivity, MSCs themselves do not activate T cells in their host or when transplanted into a recipient. This is because MSCs do not express co-stimulatory molecules e.g. CD40/CD40L and B7-1 or B7-2 [69] meaning that they cannot activate T cell responses. Further, MSCs can escape lysis by cytotoxic T cells and NK cells making them ideal candidates for cellular therapy [70].

5.3. Therapeutic uses of MSCs and mechanisms of recruitment to tissue

MSCs have potential uses within the field of transplant therapy, due to their ability to self renew and differentiate into a range of cell types, and because of their immunomodulatory effects. Many studies have been performed with MSCs to establish their therapeutic utilities. Following transplantation, allogenic MSCs have been detected in recipients at extended time points confirming their lack of immune recognition [60]. Because they don't elicit an immune response, once harvested they can be infused into either autologous or allogenous hosts without rejection, meaning the recipient need not be given immunosuppression [69]. These properties have made MSCs ideal candidates for use in the prevention of rejection of solid organ or HSC transplants and of graft verses host disease [71], as well as in the treatments of myocardial infarction [72] and ostegenesis imperfecta [73].

Significant questions remain to be answered before MSCs can be used therapeutically to their best ability; what is the best method of delivery of these cells? How do they get to the sites of injury? And how do they exert their clinical effect? Firstly, MSCs have been used therapeutically by local administration of *ex vivo* expanded cells, but systemic administration of MSCs has proven to be more difficult because the number of MSCs that home to the site of the injury is very low [74]. Determining where MSCs migrate is a crucial step in developing MSC therapies and studies have shown that after systemic infusion there are very few MSCs in the bone marrow indicating that they home to other tissues or organs. It has also been shown, in rats, that a large proportion are trapped within the lungs and liver [75], but that administration of a vasodilator significantly altered where the MSCs migrated to by allowing them to escape capture from the lungs. Other models

[76], [77] have shown that there is very little or no trafficking of MSCs to sites of undamaged tissue, therefore showing that MSCs are selectively recruited to sites where therapeutic intervention is required [78]. Also, Langer et al [79]showed that induction of vascular injury in vivo resulted in increased recruitment of injected MSCs. This suggests that MSC trafficking to sites of injury is part of the natural healing response and that administration of the patients own or donor MSCs to sites of injury can enhance the reparative response.

Although the sites to which MSCs are recruited are now better established, the mechanisms by which MSCs are mobilized into the circulation, undergo recruitment and transmigrate across the endothelium are not yet fully understood. Leukocyte homing in response to inflammatory stimuli is well known and HSC recruitment has been suggested to occur via a mechanism similar to that of leukocytes. Looking at the mechanisms by which HSCs are recruited may give an idea of what mechanisms are involved in MSC recruitment. HSCs and leukocytes employ a large proportion of similar processes such as the use of L- and E- selectin during the initial capture and rolling stages. But MSCs do not express L- selectin on their surface and the role of E-selectin is still to be determined [80]. Also, MSCs do not express platelet endothelial cell adhesion molecule (PECAM) which has a role in transmigration across the endothelial wall for leukocytes. Observations suggest that although MSCs may utilise a similar method if migration they must use a completely different set of adhesion molecules. Ruster et al [80] showed that MSCs bind to human umbilical vein endothelial cells (HUVEC) in a similar way to peripheral blood mononuclear cells and CD34+ cells, i.e. the rapid extension of podia, followed by rolling and firm adhesion. The binding of MSCs to the HUVECs was reduced when antibody against P-selectin was used to pre-treat the endothelial cells and increased when

endothelial cells were pretreated with TNFα. The same group also showed a reduced level of binding to vessel walls in P-selectin deficient mice [80]. Since MSCs do not express the P-selectin ligand P-selectin glycoprotein ligand 1 (PSGL-1) they may express a novel ligand of their own.

The actions of those cells that do migrate to sites of injury is another subject of contention but the most popular theory is that MSCs act to repair tissue injuries by the secretion of chemokines, cytokines and extracellular matrix proteins that alter the tissue microenvironment. These secreted factors inhibit fibrosis and apoptosis and promote angiogenesis and stimulate host progenitors to divide and differentiate into functional reactive units [81].

5.4. Platelets as potential assistants in MSC recruitment

At sites of disrupted endothelium, platelets are be the first line of defence and adhere to the collagen in the sub endothelium where they prevent blood loss and initiate the healing process [79]. Platelets have been shown to aid in the *ex vivo* expansion of MSCs for use in therapies. Expansion of MSCs *in vitro* is necessary for their use in therapeutics where large quantities are required. Normally, fetal calf serum is used as a growth supplement for MSCs but if the MSCs are to be used clinically this is not possible as contact between MSCs and FCS must be kept to a minimum according to European legislation [82]. Platelets are known to secrete a number of cytokines and growth factors, and platelet lysates have been shown to be able to promote expansion of MSCs in *in vitro* culture [82]. Platelet lysates were shown to contain platelet derived growth factor (PDGF), basic fibroblast growth factor (bFGF), transforming growth factor (TGF-β) and insulin like

growth factor-1 (IGF-1) [82] as well as vascular endothelial growth factor (VEGF) and platelet derived epidermal growth factor (PDEGF). These factors are involved in chemotaxis and cellular proliferation [83].

At sites of injury or infection platelets can interact with neutrophils and monocytes as well as signal mast cells, macrophages and dendritic cells if they gain access to the extravascular space whilst also receiving signals from macrophages and mast cells in the form of platelet activating factor (PAF) showing that at sites of inflammation platelets can both supply and respond to signals [84].Activated platelets release proinflammatory mediators such as IL-1β and at sites of inflammation, circulating platelets adhere to the exposed subendothelial matrix and become activated, activated platelets are known to express P-selectin, a vascular cell adhesion molecule known to bind to P-selectin glycoprotein ligand 1 (PSGL-1) on circulating leukocytes. These interactions mediate rolling of leukocytes (Figure 5.2) followed firm adhesion, mediated by integrins and transmigration across the vessel wall [84] mediated by platelet endothelial cell adhesion molecule (PECAM).

The importance of platelet interactions with endothelium and its contribution to inflammatory events was further shown by Gawaz et al [85] who demonstrated that activated platelets modulate monocyte chemotactic protein-1 (MCP-1) secretion from the vessel wall and surface expression of intercellular adhesion molecule- 1 (ICAM-1) on the endothelium.

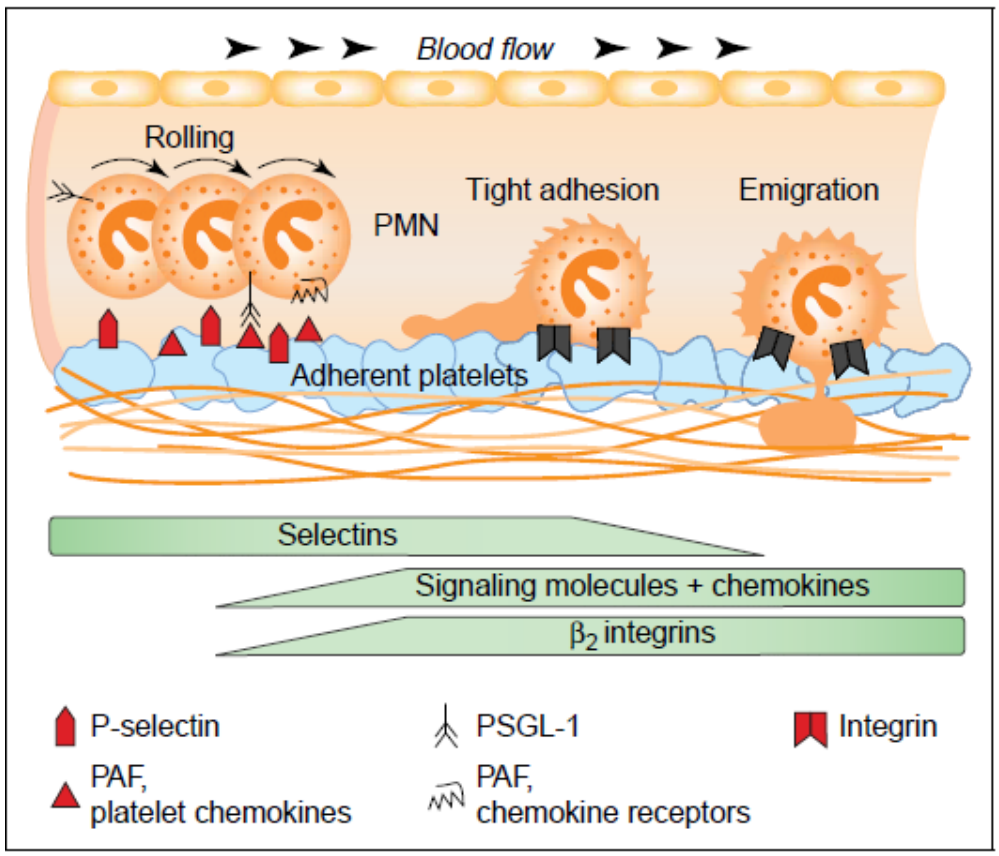

Figure 5.2. Recruitment of leukocytes from the circulation is mediated by platelet interactions.

P selectin on platelets binds to p selectin glycoprotein ligands on Polymorphonuclear leukocytes (PMNs; neutrophils) instigating rolling. Firm adhesion of the cells and eventual transmigration through the vessel wall is mediated by integrins and PECAM respectively. [84].

There is a small but definite presence of HSCs in circulating blood which are thought to migrate to extramedullary sites, the trafficking of these HSCs is thought to have similar mechanisms to that of leukocytes [86]. Further, HSCs were shown to traffic constitutively

to multiple extramedullary tissues where they remain for approximately 2 days before they enter the draining lymphatics and return to the blood. HSCs express multiple traffic molecules including PSGL-1, VLA-4 and LFA-1 but the exact mechanisms by which HSCs are recruited from the blood to tissues remains to be known [86], although platelets have been shown to play a role in the adhesion of HSC to endothelium. Janowska-Wieczorek et al [87] showed that when HSCs are covered with platelet microparticles their adhesion to endothelium is increased as is the speed by which the engraftment occurs indicating that platelet microparticles are involved in both adhesion and homing of HSCs. It is thought HSCs may follow trafficking patterns similar to leukocytes when they are homing to the bone marrow, involving similar rolling, firm adhesion and transmigration events. Frenette et al [88] discovered that homing of HSCs is regulated primarily by P and E selectins and to a lesser extent vascular cell adhesion molecule (VCAM-1). It is unclear however which ligands on the HSCs bind to P or E selectin on the vasculature. Activated platelets have been shown to increase the migratory abilities of vascular smooth muscle cells and endothelial cells which are important in repair of vessel walls [89].

Whilst the interactions between platelets and leukocytes and platelets and HSCs have been investigated the interactions between platelets and MSCs have not. Since platelets have clear roles in the trafficking and migration of leukocytes and HSCs and their progenitor cells, they may also be involved in the trafficking of MSCs. It may be possible that platelets recruit MSCs to sites of injury where they induce them to differentiate and participate in the restoration of damaged tissue.

5.5. Hypothesis

The mechanisms by which MSC are recruited to sites of injury are not well defined. Recent studies show that platelet lysates help in the growth and differentiation of MSCs and others indicate that P-selectin may be involved in the process of capture of the MSCs and aid their rolling along the surface of endothelium. Since platelets express P-selectin when activated, we hypothesised that they may bind to MSCs in the peripheral blood circulation or to the wall of damaged vessels, and aid in recruitment of MSC to the vessel wall.

5.6. Aims

We aimed to determine if platelets bind to MSCs in whole blood and platelet rich plasma under normal conditions and upon the addition of the platelet activating agent TRAP. In parallel, we aimed to use flow based assays to determine if flowing MSCs in blood could bind to model capillaries coated with collagen (a platelet-binding surface) or purified P-selectin.

6. Materials and Methods

6.1. Methods

Blood Collection

Blood was collected from consenting adults into tubes containing either Citrate Phosphate Dextrose Adenine (CPDA; Sigma) at a ratio of 1:7 or the peptide thrombin-inhibitor PPACK (Sigma), at a concentration of 40μM and mixed. Samples were used within 2h of withdrawal.

Platelet Rich Plasma

Platelet rich plasma (PRP) was made from whole blood by centrifuging at 200g for 5minutes, after which the plasma layer was collected.

Mesenchymal stem cell culture

Mesenchymal stem cells were purchased (Lonza) at passage 2. The cells were thawed and seeded onto 75cm^3 flasks (T75) which had been pre coated with fibronectin (1μg/ml). Cells were grown in Mesenchymal Stem Cell Basal Medium (MSCBM; Lonza) with additional Mesenchymal Cell Growth Supplement (MCGS), L-glutamine, and GA-1000 antibiotic (Lonza) (Complete culture medium). Complete medium was renewed every 4 days. Cells were grown at 37^oC in 5% CO_2. Cells were grown to ~ 90% confluence before being passaged. MSCs were removed from the surface of the flask to enable them to be passaged or used in an experiment, cells between passage 7 and 9 were used for experiments. The culture media was removed from the flask and the cells rinsed in 2ml EDTA (0.5mM; Sigma®) for 1-2 minutes to remove calcium and magnesium. The EDTA

was aspirated and cells were dissociated by the addition of 2ml of trypsin (1x; Sigma®) to the flask followed by incubation at 37^{o}C/5% CO_2 for 5-10minutes until the cells appeared round when viewed under the light microscope. The flask was then firmly tapped to fully dissociate the MSCs before 8ml complete culture medium was added. The medium plus MSCs was centrifuged at 300g for 5 minutes. The supernatant was then discarded and the cell pellet was resuspended in 1ml of complete culture medium. If cells were to be passaged, another 2ml of medium was added to the cells giving a total of 3ml. This was split into 3x 75cm^3 flasks each containing 7ml of complete culture medium. For assays, cells were held in 1ml of medium and their concentration measured using a Nexcelom Cellometer cell counter (Biosciences); 20µl of MSCs was added to a Nexcelom slide and placed into the microscope reader. The concentration was determined as cells/ml.

Flow Cytometry to analyse platelet binding to MSC in blood or PRP

MSCs were harvested and diluted to a standard concentration of 1x 10^6/ml in complete culture medium. When MSCs were to be analysed on their own, 100µl aliquots were added to polypropylene FACS tubes to be stained. When adding the MSCs to blood, they were mixed at a ratio of 1:9 in bijoux tubes containing a flea on a magnetic stirrer. Alternatively MSCs were added in the same ratio to PRP. Whole blood or PRP was stirred for either 5minutes or 15minutes before 100µl aliquots were removed and added to polypropylene FACS tubes to be stained. In some cases, thrombin receptor activating peptide (TRAP; Tocris Biosciences) was added to the blood/PRP and MSC mix (20µM) before stirring commenced; 100µl aliquots were taken after 5 minutes sand 15 minutes and stained along side the other samples.

Samples were stained with appropriate antibodies against antigens identifying MSC (CD105), platelets (CD42b) or leukocytes (CD45) (Table 2.1) for 30minutes in the dark at room temperature, after which 2ml FACS lyse (BD Biosciences) was added to each sample and left for 10minutes in the dark at room temperature. Samples were centrifuged at 300g for 5minutes at room temperature and supernatants were poured off, pellets were washed in 2ml phosphate buffered saline (PBS; Sigma) containing no Calcium or Magnesium plus 0.5% albumin (Sigma) (0.5%PBSA), centrifuged and supernatant poured off. Pellets were washed again in 0.5% PBSA- and pellets were finally resuspended in 500µl of 2% formaldehyde in PBS. Samples were read of on the FACS Cyan flow cytometer.

Antibody	**Flourophore**	**Concentration used**	**Company**
CD105	FITC	1:200	Ancell 326-040
CD42b	PE-CY5	1:10	BD Pharmingen 551141
CD45	FITC	1:100	ImmunoTools 21270453

Table 6. 1. Antibodies used the fluorophores they were conjugated to and the concentrations they were used at.

FACS analysis.

Flow cytometry data was analysed by Summit v4.3 software. The forward scatter/side scatter plot was used to distinguish the MSC population which was gated around; the gate was applied to the subsequent plots when desired. Fluorescence intensity Plots used to analyse the data included CD105-FITC /CD42b-PE-Cy5 and FITC and PE-Cy5 alone. Using the CD105/CD42b plot, quadrants were used to determine CD105 positive and CD42b positive cells. The quadrants were set at 5.27 for CD105- FITC and 22.34 for CD42b- PE-Cy5; any cell falling within quadrants 1 and 2 was said to be PE-Cy5 (CD42b) positive and any cell falling within quadrants 2 and 4 was said to be FITC (CD105) positive, any cell falling with quadrant 2 was classed as being double positive. For

analysis; cells that fell with quadrant 2 were taken as a percentage of cells that fell within quadrants 2 and 4 combined.

Flow-based Assay of MSC adhesion in flowing blood

For the flow assay, MSCs were dissociated and stained with Cell Tracker Green (Invitrogen); 5µl was added to 10ml culture medium (5µM) with no added supplements and to which the MSCs were added and left to incubate at 37^{o}C/5% CO_2 for 30minutes. The cells were centrifuged at 300g for 5minutes and the medium removed, and the cells were resuspended in 10ml of complete culture medium and allowed to incubate for a further 30 minutes. Finally the cells were centrifuged, the supernatant was removed and the cells were resuspended in 1ml of medium for the concentration to be measured. The cells were diluted to a final volume of 1x 10^6/ml and added to blood.

Glass capillary slides (microslides) with rectangular cross section 3mm x 0.3mm and length 5mm were coated by drawing 50µl of the appropriate coating protein solution into the slide with a pipette followed by incubation at 37^{o}C/ 5% CO_2 for 1 hour. The slides were washed and remaining protein-binding sites were blocked with PBS containing 1% albumin for 2 hours at 37^{o}C/5% CO_2. Slides were coated in either P-selectin (10µg/ml; R&D systems) or type I collagen (500µg/ml; Horm collagen; Axis-Shield) or albumin alone.

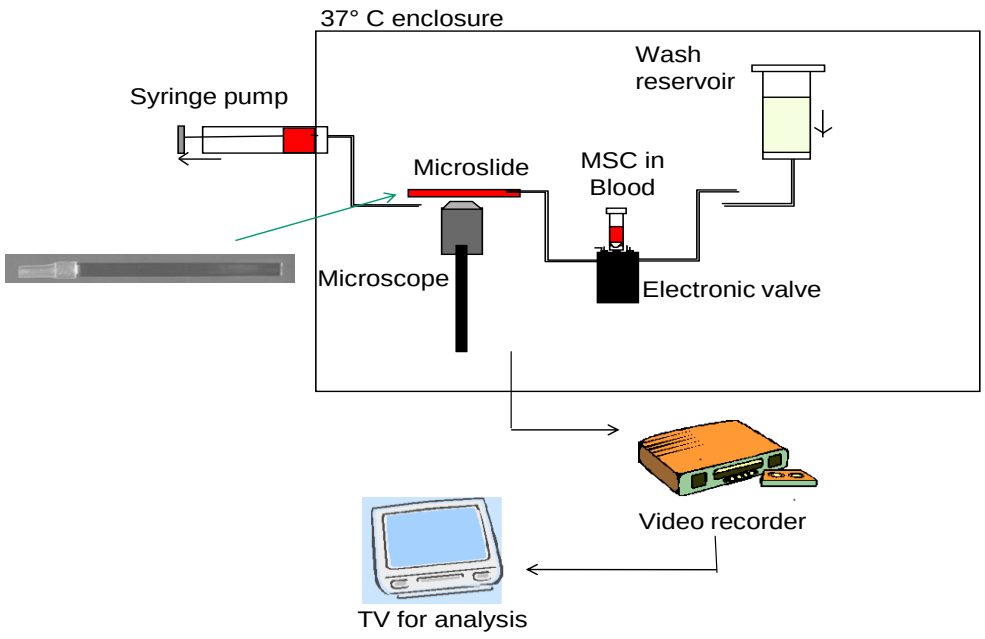

Figure 6.1. Diagrammatic representation of the flow assay.

Samples were pulled through the microslide by a syringe pump, the flow of MSCs were captured by video and displayed on the television for analysis.

The flow assay is shown diagrammatically in figure 2.1. The coated microslide was placed under the microscope having been glued to a glass slide to hold it into place. Double sided sticky tape was wrapped around either end of the microslide and silicon rubber tubing was attached. One end was connected to a syringe pump (Harvard apparatus) and the other was connected to a valve which could be switched between reservoirs holding the test sample or PBS. Initially PBS without Ca or Mg was flushed through the system, and then the test sample was perfused for 5 minutes at a flow rate (0.181ml/min) chosen to provide a wall shear rate of $70s^{-1}$.

The test sample was 2ml blood collected into either CPDA or PPACK for the flow assay, to which 200ul fluorescent-labelled MSCs were added MSCs flowing through the microslide were viewed by the fluorescence microscope equipped with a CCTV camera and images recorded with a video recorder.

Flow assay analysis.

Behaviour of mesenchymal stem cells was analysed by watching the video tape of the flow assay, examining recordings of approximately 30 seconds made at10 different fields along the centreline of the microslide for each condition. First, the video playback of a field was stopped and the number of MSCs in view on the screen was recorded; next a line was drawn down the middle of the screen and the number of MSCs flowing past that line in 1 second was counted (Flux). Finally the time MSCs took to cross the screen of the television was recorded. The size of the screen was measured using a microscope stage micrometer viewed by the CCTV camera. From the above, the following were calculated:

1. The number of cells in view was converted to the number of cells per mm^2 at the wall of the microslide.
2. The number of MSCs flowing past the line in 1 second (Flux) was converted to the percentage of total cells flowing past.
3. The time it took MSCs to cross the screen was converted to velocity (μm/s).

7. Results

7.1. Binding of platelets to MSC in stirred blood

Firstly the antibody concentrations needed for the assay had to be determined. This was achieved by staining 100µl aliquots of MSCs with anti CD105-FITC antibody at differing concentrations; 1/50, 1/100 and 1/200 (Figure 7.1) and staining blood for platelets with anti CD42b-PE-Cy5 antibody at differing concentrations; 1/5, 1/10 and 1/20. MSCs were tested alone and mixed 1:10 in whole blood; blood was also tested alone without the additions of MSCs. Unstained samples were also tested Figure 7.1). These titration experiments showed that the concentration of anti CD105 antibody that was sufficient for use was 1/200 as the level of fluorescence at this concentration was the same as at a concentration of 1/50. The concentration of anti CD42b antibody that was sufficient for use was 1/10 because the level of fluorescence at this concentration was the same as that at 1/5 but levels decreased when a concentration of 1/20 was used.

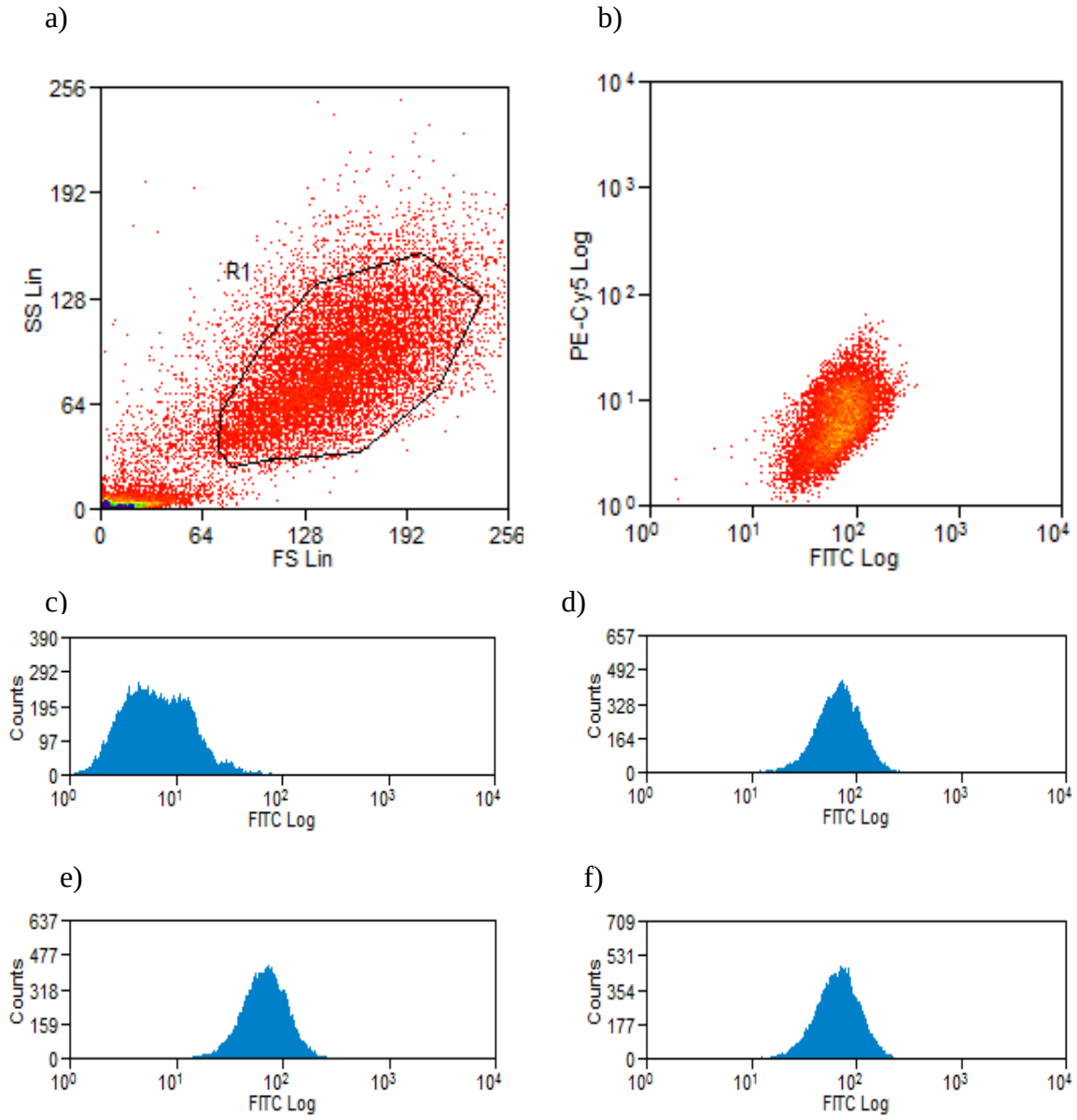

Figure 7.1. MSCs stained with CD105-FITC at different concentrations.

a) MSCs alone stained with CD105-FITC were gated around.

b) The position of MSCs stained with CD105-FITC is shown on the FITC/PE-Cy5 graph

c) The position of unstained MSCs is shown on the FITC histogram.

d) MSCs stained with CD105- FITC at 1/50 concentration.

e) MSCs stained with CD105- FITC at 1/100 concentration.

f) MSCs stained with CD105- FIITC at 1/200 concentration.

Next, MSCs were mixed with whole blood (CPDA) or PRP in bijoux tubes at a ratio of 1:10 and stirred; 100µl samples were removed after 15minutes and stained with both CD105 and CD42b using the concentrations of antibodies determined above. In a separate bijoux tube, TRAP a platelet activator was added to the blood/MSC mixture and again 100µl samples were taken and stained for both CD105 and CD42b. MSC or blood samples alone were also stained for either CD105 or CD42b respectively, or left unstained. With the scatter plots obtained from these samples it was possible to determine where the MSCs lie on the forward scatter/ side scatter plot when sampled alone and when mixed with whole blood. Further, it was possible to set boundaries to classify cells as being either positive or negative for CD42b and/or CD105 as illustrated in figure 7.2.

Using the forward scatter/ side scatter plot the MSC population was determined by eye and gated around; this gate was applied to all subsequent plots including a CD105/CD42b plot and CD105 and CD42b histograms (Figure 7.2). Using the CD105(FITC)/CD42b(PE-Cy5) plot, quadrants were applied so that 99% of cells were within the quadrants defined as being negative when they were unstained and in quadrants defined as being positive when stained. The percentage of cells in each of the resulting quadrants was used to determine how many cells were CD105 positive and CD42b positive; cells within quadrants R2 and R3 were classed as being CD42b positive, i.e. platelets. Cells within quadrants R3 and R5 were classed as CD105 positive, i.e. MSCs, those cells with R3 were said to be double positive i.e. MSCs with platelets bound, and those cells within quadrant R1 as being double negative, i.e. neither MSCs nor platelets. The number of MSCs that were double positive was worked out as being the number of cells within R3 as a percentage of cells within R3+ R5.

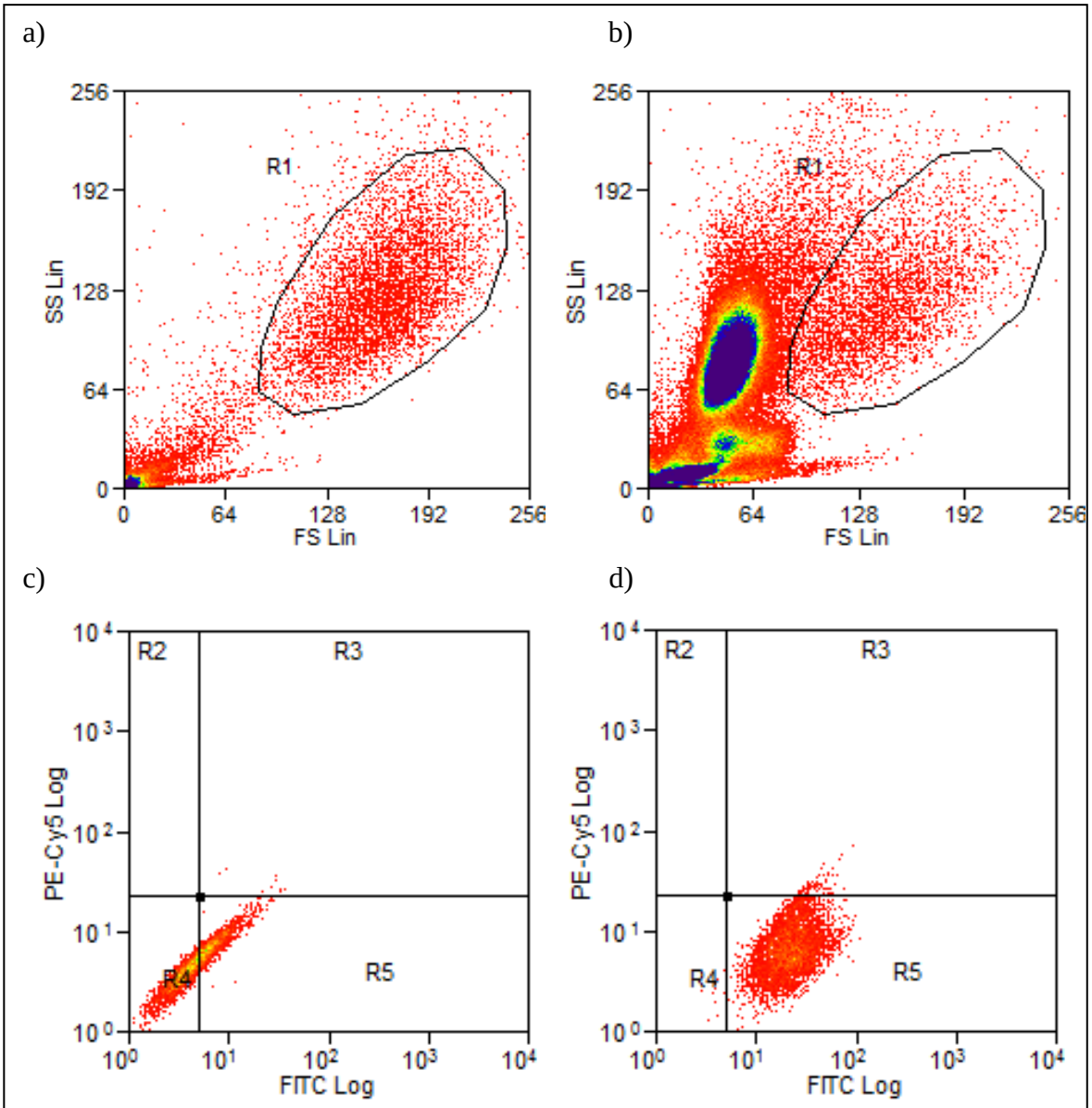

Figure 7.2. FACS plots of MSCs.

a) Forward scatter/side scatter plot for MSCs alone. MSC population is gated.

b) Forward scatter/side scatter plot for MSCs in whole blood. MSC population is gated.

c) CD105/CD42b plot of unstained MSCs.

d) CD105/CD42b plot of MSCs stained with CD105- FITC and CD42b- PE-Cy5.

Using the boundaries described, results for the experiment also described above showed that MSCs mixed with blood gave a similar number of double positive cells (4.1%) as MSCs with PRP (4.6%), whilst the addition of platelet activator TRAP reduced the number of double positive cells in whole blood to 1.5%. MSCs alone gave a background level of CD42b staining of 0.5%.

Following this, experiments were conducted with varying conditions to identify differences in MSC and platelet binding between the conditions. The effects of anticoagulant used were tested by stirring MSCs with blood that was collected into either CPDA a calcium chelator which prevents the coagulation cascade from occurring, or PPACK a thrombin inhibitor. The effects of time were tested by stirring blood and MSC mixtures for either 5 minutes or 15 minutes and the effect of platelet activation was tested by adding TRAP to the blood and MSC mixture. MSCs were also mixed with PRP instead of whole blood in some experiments. The percentage of cells that were double positive for CD105 and CD42b were calculated as above and the averages of the data retrieved were used to compare the different conditions ; standard error of the mean (SEM) was also calculated and error bars added to the graph (Figure 7.3).

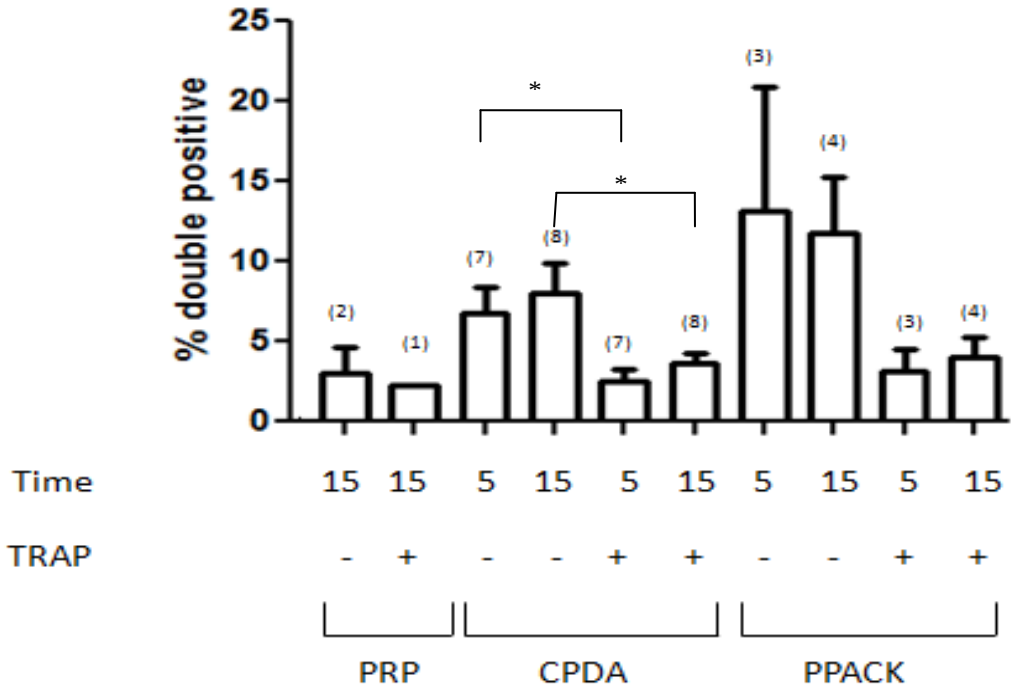

Figure 7.3. Percentage double-positive particles when MSCs were mixed with either CPDA or PPACK blood or PRP for 5 minutes or 15 minutes, +/- TRAP.

Data are the mean +/- SEM from (n) experiments. Number in brackets above the bars indicates the number of repeats performed for that condition. * Indicates a significant difference (<0.05) in a paired T test in samples with/without TRAP.

The average percentages show that overall there is a greater number of CD105 and CD42b double positive cells within the MSC gate when they are mixed with PPACK blood than with CPDA blood with e.g. 13.2% in the PPACK blood after 5 minutes compared to 6.7% in CPDA blood after 5 minutes. But an unpaired T test showed that there was no significance between these results. The results also show that time has only a slight effect on the binding of platelets to MSCs, with the number increasing slightly between 5 to 15 min for most conditions except in PPACK blood, not surprisingly, changes in time do not

produce significant results in unpaired T tests. Surprisingly, the addition of TRAP to the blood and MSC mixtures to activate platelets reduced the levels of CD105/CD42b double-positive cells in both CPDA and PPACK blood to 2.5% and 3.1% respectively after 5 minutes. The difference in the percentages of double positive cells between CPDA blood after 5 minutes and CPDA blood plus TRAP after 5 minutes were significant when using a paired T test to analyse the results with a p value of 0.0185. There was also a significant difference after 15 minutes in CPDA blood between samples that had not had TRAP added and those that did ($p= 0.0244$). The differences in PPACK blood before and after addition of TRAP were not significant, possibly because of the large standard error bars. The results also illustrate that mixing MSCs with blood provides more double positive cells than MSCs mixed with PRP, although upon the addition of TRAP to PRP the levels of binding between MSCs and platelets decreased, showing the same pattern as in whole blood. The average levels of background fluorescence (Figure 7.4) were low, at less than 1% showing that the levels of fluorescence obtained from samples were true readings.

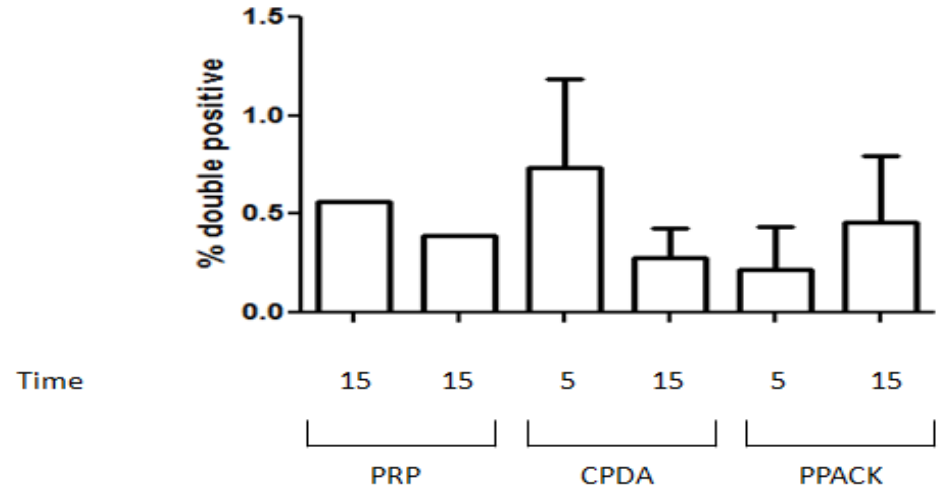

Figure 7.4. Percentage background fluorescence when MSCs were mixed with either CPDA or PPACK blood or PRP for 5 minutes or 15 minutes and were left unstained.

The level of background fluorescence in unstained samples was less than 1% in most samples.

We checked whether any cells within the MSC gate were in fact leukocytes, e.g. aggregated with platelets. Samples (using CPDA blood alone) were stained with CD45-FITC, a leukocyte marker. The FACS data were analysed as for staining with CD105 and the results illustrated that there were very few cells within the MSC gate that were positive for CD45, with stained samples having no more fluorescence than unstained samples, indicating that platelets within this gate were not binding to leukocytes (Figure 7.5)

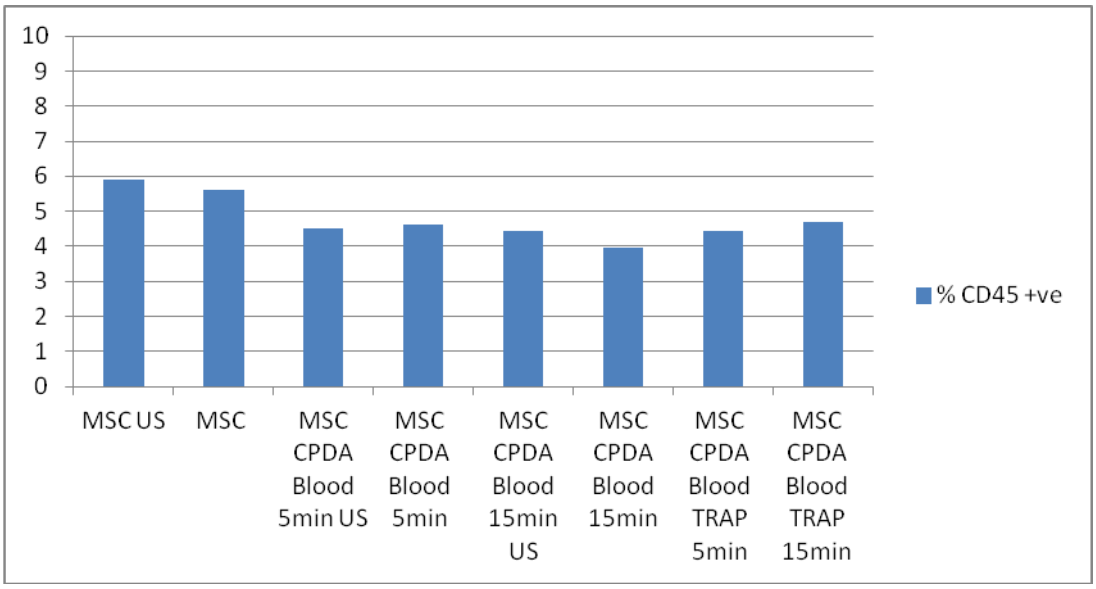

Figure 7.5. The percentage of cells within the MSC gate that are positive for CD45. The number of CD45 positive cells within the MSC gate is no larger in stained samples than in unstained samples showing that there are no CD45 positive cells within this gate. US= unstained.

7.2. Behaviour of MSC perfused across adhesive surfaces in blood.

The MSCs were stained with cell tracker green to enable them to be viewed under a fluorescent microscope; they were then added to either CPDA or PPACK blood at a ration of 1:10. Samples were then flowed through microslides coated in albumin, collagen or P selectin and recorded onto video tape. The video tape were analysed to obtain the number of cells near the wall per mm^2, the flux of the cells near the wall as a percentage of the total perfused, and the velocity of the cells in μm/second. Averages were compared for CPDA vs. PPACK as anticoagulants, and for surfaces coated with albumin vs. collagen vs. P selectin, standard error bars were also added to graphs.

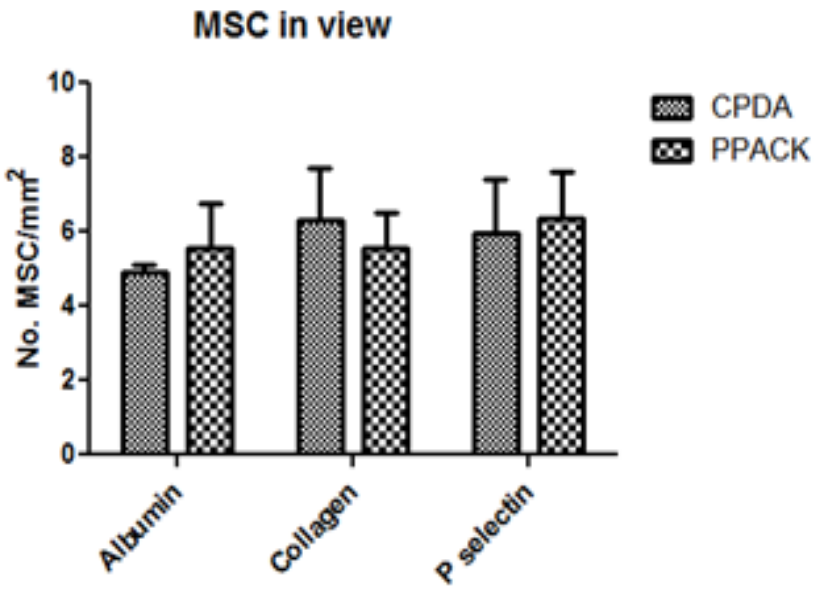

Figure 7.6 Effect of anticoagulant and adhesive substrate on the number of MSCs per mm^2.

The number of MSCs in view on the screen was converted into number of MSCs per mm^2.There was little difference in the number of cells per mm^2 between samples of MSCs in CPDA or PPACK blood when flowed over surfaces of albumin, collagen or P selectin.

Figure 7.6 shows that there was little difference in the numbers of MSCs in view between the different proteins used to coat the microslides and between the anticoagulant used in the blood. Two way ANOVA revealed there were no significant effects of anticoagulant or surface on the number of MSCs in view.

The number of cells flowing past an arbitrary line on the screen (flux) in 1 second was counted, and converted into the percentage of the total number of cells perfused. Averages of the resulting percentages were used; the resulting figures were plotted onto graphs comparing CPDA to PPACK and albumin to collagen and P selectin (Figure 7.7).

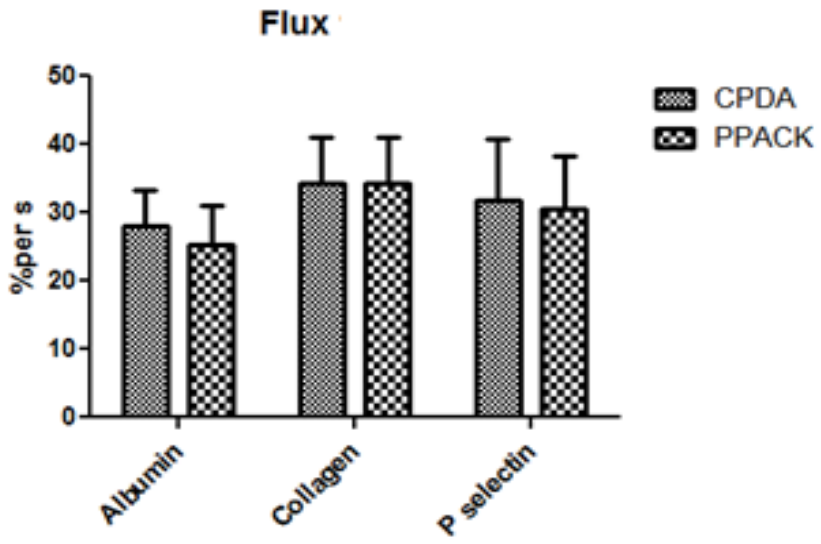

Figure 7.7 Effect of anticoagulant and adhesive substrate on percentage of cells flowing past per second.

The number of cells flowing past an arbitrary line per second was converted into the percentage of the total cells flowing past according to the flow rate used for the assay. There was very little difference in flux between samples of MSCs in CPDA or PPACK blood when flowed over surfaces of albumin, collagen or P selectin.

The differences in flux between the types of surface and the anticoagulants used are very small. There were a slightly larger percentage of cells flowing close to the walls in microslides coated with collagen and P selectin than albumin but the error bars for all conditions were also quite large, and there was very little difference between the use of CPDA or PPACK. None of the differences were significant when ANOVA was used to analyse them.

The time it took for MSCs to cross the screen was converted into velocity; averages of the 10 fields viewed per condition were used to compare the samples. The figures obtained were plotted onto graphs comparing CPDA to PPACK and albumin to collagen and P selectin again (Figure 7.8).

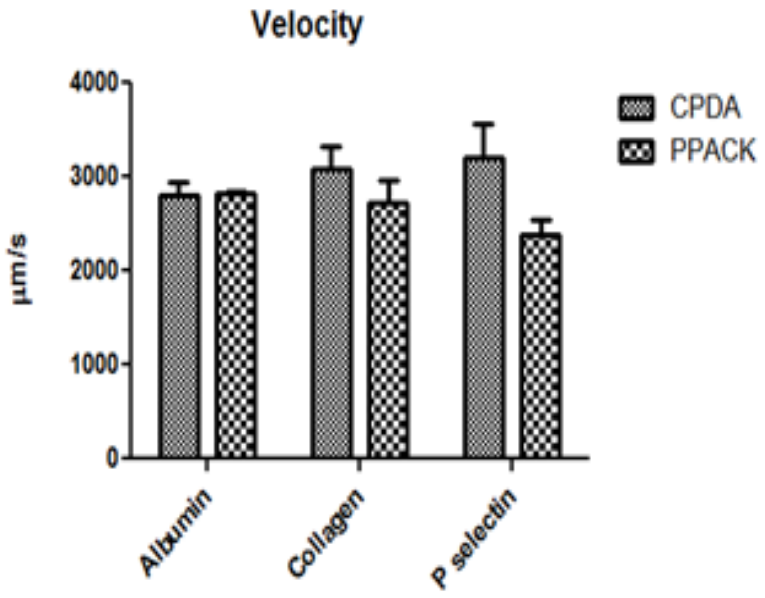

Figure 7.8. Effect of anticoagulant and adhesive substrate on the velocity of MSCs flowing through microslides.

The time it took MSCs to cross the screen was converted to velocity. There was very little difference in velocity between samples of MSCs in CPDA or PPACK blood when flowed over surfaces of albumin, collagen or P selectin.

Again the differences between the samples are small but the biggest differences are between CPDA and PPACK blood on a P selectin surface with PPACK having a lower velocity than CPDA. Two way ANOVA showed no significance between the results.

8. Discussion

8.1. Binding of platelets to MSC in stirred blood.

Experiments performed have shown that a small proportion of platelets within the blood can bind to mesenchymal stem cells, under the right conditions. Cultured mesenchymal stem cells were harvested and stirred with whole blood, collected into either CPDA or PPACK anticoagulants, or stirred into platelet rich plasma (PRP). Samples were stirred for 5 or 15 minutes before being stained with MSC marker CD105 and platelet marker CD42b and being analysed by flow cytometry. The effect of platelet activation was tested by the addition of TRAP, a platelet activating peptide, in some of the samples tested. Multiple repeats of experimental conditions were performed and the average results obtained were used to compare the effects of anticoagulant, time and platelet activation.

The type of anticoagulant used seemed to have a small effect on the levels of double positive cells in samples, with MSCs mixed with PPACK blood having higher levels of platelet/MSC aggregates compared to CPDA blood after both 5 minutes and 15 minutes. Although the results obtained from CPDA blood were much more consistent with lower standard errors in CPDA blood than PPACK blood. The length of time that MSCs were mixed with blood had differential effects depending on which anticoagulant the blood was collected into, with the amount of double positive cells increasing after 15 minutes in CPDA blood but decreasing after 15 minutes in PPACK blood showing that more repeats are needed to fully determine the effects of time.

Thrombin receptor activating peptide, TRAP is a synthetic peptide which mimics many of the effects of thrombin [90], it has been shown to stimulate platelet activation as well as

induce aggregation, ATP release and phospholipase C activity [90]. The experiments have shown that this peptide has a large effect on the binding of platelets to MSCs with the levels reduced upon addition of TRAP to the MSC/ blood mixtures. This may be because as the platelets are activated they either form platelet aggregates or bind to lymphocytes and leukocytes rather than to MSC. On this assumption, when MSCs were mixed with PRP which contains fewer leukocytes than whole blood, the levels of binding within the MSC gate would be expected to increase after the addition of TRAP because the platelets would have fewer leukocytes to bind to outside of the MSC gate. This was not the case; the levels of binding when MSCs were mixed with PRP were lower than in whole blood before the addition of TRAP, and in samples to which TRAP was added the levels of binding were decreased like they were in whole blood samples. To ascertain if platelets were binding to leukocytes within the MSC gate the levels of leukocytes present on the MSC gate was determined by staining samples with CD45 a leukocyte marker. The resulting FACS data revealed that there was no more fluorescence in samples stained with CD45-FITC than those left unstained illustrating that leukocytes are absent from the MSC gate. This therefore showed that within the MSC gate platelets are binding to MSCs or have formed platelet aggregates that are of similar size to MSCs.

The above data has demonstrated that small levels of platelets are able to bind MSCs under appropriate conditions but that activated platelets are less likely to bind to MSCs. Since platelets are activated in response to injury or inflammation which is the time when MSCs are most prominent in the blood the results would suggest that platelets do not aid recruitment of MSCs in response to injury.

Future work

Given the large error bars for some conditions, it would be desirable to carry our more repeats of each condition to fully determine effects of anticoagulant, time and activation.

8.2. Behaviour of MSC perfused across adhesive surfaces in blood.

MSCs were also analysed using a flow based system which simulates the flow of blood within vessels. MSCs were stained with cell tracker green and were mixed with whole blood collected into CPDA or PPACK anticoagulants. Samples were flowed through microslides coated with albumin as a control, or collagen or P selectin. Collagen was chosen because it is exposed upon injury to blood vessel walls and P selectin was used because previous studies have indicated that it aids in the recruitment of MSCs [80]. The flow of MSCs in blood was recorded on video tape which was used for analysis to determine if there were any differences between the surfaces and which anticoagulant the blood was collected into. Per condition i.e. PPACK or CPDA and albumin, collagen or P selectin 10 frames were viewed, in each of these frames the number of cells in view at the start was counted, the area in view was also determined and from this the number of cells per mm^2 was deducted. There was little difference between the averages between the different conditions and two way ANOVA revealed no significance between the different conditions. Also calculated from the video recording was the flux of the cells, this was calculated from the number of cells that crossed the screen in 1 second which was converted to a percentage of the total number of cells flowing through the microslide as the cells that were in view were cells that were near the microslide wall and not the total number of cells flowing through. The average results obtained from 5 experiments for each condition were used to compare the conditions. The highest percentage was from CPDA

blood flowed over a collagen surface and was 33.21% of the total cells, the lowest percentage was from PPACK blood flowed over albumin which gave a percentage of 26.43%. The difference between the highest and lowest percentages shows that the range between the condition types is narrow and analysis of these results showed that there were no significant differences between the conditions. The velocity of the MSCs was also calculated from the video tapes by counting how long it took for cells to cross the screen. Those MSCs that may have been adhering to the surface would have had a lower velocity (μm/s) than those that were not, also it would be expected that the velocity of cells flowing through microtubes coated in collagen or P selectin would be lower than albumin which was a control that MSCs are not expected to adhere to. But the velocity of cells in CPDA blood was quicker when flowed over collagen and P selectin than albumin which shows no adhesion between MSCs and the surfaces. The velocity of MSCs in PPACK blood was similar between albumin and collagen but was reduced when flowed over P selectin, but like the results obtained for the other parameters the range between the averages of the different conditions is small. Also, like the other parameters used to analyse the results, the two way ANOVA revealed no significance in the results.

The results obtained from the flow assay suggest that MSCs do not adhere to collagen or P selectin. The latter does not agree with the findings of Ruster et al. who found that binding of MSCs to HUVECs was reduced when antibody against P selectin was used. Those studies were carried out using isolated MSC whereas this study used MSC suspended in blood, which is closer to the situation in vivo.

Future Work

The flow assays were performed 5 times over collagen and P selectin but only 4 times over albumin so would need to be repeated many more times to confirm that MSCs do not bind to either of them. It would be interesting to determine if platelet activation had an effect in this experimental setting by the addition of TRAP to the samples before they are flowed over the microtubes. It may also be worth coating the microslide with different molecules, for example E selectin or VCAM-1 to ascertain is they are able to support binding of MSCs.

9. Appendix

Primer sequences used for PCR

	Primer Sequence	Restriction site	Length of product
Amigo1 forward	5'GATCGAATTC|ATG|CA CCCCCACCGTGACCCG 3'	EcoR1	1476bp
Amigo1 reverse	3'AGACTATGCGGGTAA CACCACGAGCTCCTAG 5'	Xho1	1476bp
Amigo2 forward	5'GATCGGATCC|ATG|TC GTTACGTGTACACACT 3'	BamH1	1569bp
Amigo2 reverse	3' TGTGGAAAACACCGC AGGTGAGAGCTCCTAG 5'	Xho1	1569bp
Amigo3 forward	5'GATCGGATCC|ATG|AC CTGGTTGGTGCTGCTG 3'	BamH1	1509bp
Amigo3 reverse	3'AGGCTCCCAGGGTAC TGTTGGGAGCTCCTAG 5'	Xho1	1509bp
Lingo1 forward	5'GATCGGATCC|ATG|CA GGTGAGCAAGAGGATG 3'	BamH1	
Lingo1 reverse	3' TTCAAGTTGTACTTC TACTATGAGCTCCTAG 5'	Xho1	
NgR forward	5'GATCGAATTC|ATG|AA GAGGGCGTCCGCTGGA 3'	EcoR1	1461bp
NgR reverse	3'TGTCACGAACCCGGG ACGACTGAGCTCCTAG 5'	Xho1	1461bp
p75 forward	5'GATCGAATTC|ATG|GGG	EcoR1	1323bp

	GCAGGTGCCACCGGC 3’		
p75 reverse	3’TGACGGTGTAGGGGCC ACACTGAGCTCCTAG 5’	Xho1	1323bp

Restriction sites that were incorporated into the primers are highlighted in red, start codons are boxed and stop codons are underlined.

Internal primer sequences used for DNA sequencing

Name	Primer sequence
hAmigo1 int 1	5’ATGGCCCAGCTGCAGAAA 3’
hAmigo1 int 2	5’AACGGGTGCTAGATGAGG 3’
hAmigo2 int 1	5’TATGTTGGAAGGTTCAAG 3’
hAmigo2 int 2	5’GAAAGCCCTCGTTTTGAG 3’
hAmigo2 int 1-2	5’ TATGTTGGAAGGTTCAAG 3’
hAmigo3 int 1	5’ACGAGCATGCCTTCCACG 3’
hAmigo3 int 2	5’ATAGGCAACGTACAGGAG 3’
hNgR int 1	5’ATGACACCTTCCGCGACC 3’
hNgR int 2	5’TTACCATCCCATCTGGAC 3’
hp75 int 1	5’TGTGCGAGGACACCGAGC 3’
hp75 int 2	5’AGAAAAACTCCACAGCGA 3’

Primer sequences used for overlap extension PCR

hAM1HA OLF	5’ GATGTTCCAGATTATGCTGGCCGAGCCGTGGTT AGC 3’
hAM1HA OLR	5’ GCTAACCACGGCTCGGCCAGCATAATCTGGAAC ATC 3’
hAM1 rev	5’ GATCCTCGAGTCACACCACAATGGGCGTATC AGA 3’
hAM2HA OLF	5’ GATGTTCCAGATTATGCTGTGTGCCCCACCGCT TGC 3’
hAM2HA OLR	5’ GCAAGCGGTGGGGCACACAGCATAATCTGGAAC ATC 3’
hAM2 rev	5’ GATCCTCGAGTTAAGTGGACGCCACAAAAGG TGT 3’
hAM3HA OLF	5’ GATGTTCCAGATTATGCTACCCCGGACTCCGAG GGT 3’
hAM3HA OLR	5’ ACCCTCGGAGTCCGGGGTAGCATAATCTGGAAC ATC 3’
hAM2 rev	5’ GATCCTCGAGCTAGGTTGTCATGGGACCCTC GGA 3’
hNgRHA OLF	5’ GATGTTCCAGATTATGCTTGCCCAGGTGCCTGC GTA 3’
hNgRHA OLR	5’ TACGCAGGCACCTGGGCAAGCATAATCTGGAAC ATC 3’
hp75HA OLF	5’ GATGTTCCAGATTATGCTAAGGAGGCATGCCCC ACA 3’
hp75HA OLR	5’ TGTGGGGCATGCCTCCTTAGCATAATCTGGAAC ATC 3’
HAEco FOR	5’ GATCGAATTCATGTCTGCACTTCTGATCCTA 3’
HABamHI FOR	5’ GATCGGATCCATGTCTGCACTTCTGATCCTA 3’

10. References

1. Fawcett, J.W. and R.A. Asher, *The glial scar and central nervous system repair.* Brain Research Bulletin, 1999. **49**(6): p. 377-391.
2. Filbin, M.T., *Myelin-associated inhibitors of axonal regeneration in the adult mammalian CNS (vol 4, pg 703, 2003).* Nature Reviews Neuroscience, 2003. **4**(12): p. 1019-1019.
3. McDonald, C.L., C. Bandtlow, and M. Reindl, *Targeting the Nogo Receptor Complex in Diseases of the Central Nervous System.* Current Medicinal Chemistry, 2011. **18**(2): p. 234-244.
4. Carulli, D., et al., *Chondroitin sulfate proteoglycans in neural development and regeneration (vol 15, pg 252, 2005).* Current Opinion in Neurobiology, 2005. **15**(2): p. 252-252.
5. Schnaar, R.L., et al., *Myelin-associated glycoprotein and complementary axonal ligands, gangliosides, mediate axon stability in the CNS and PINS: Neuropathology and behavioral deficits in single- and double-null mice.* Experimental Neurology, 2005. **195**(1): p. 208-217.
6. Strittmatter, S.M., et al., *Myelin-associated glycoprotein as a functional ligand for the Nogo-66 receptor.* Science, 2002. **297**(5584): p. 1190-1193.
7. Wang, K.C., et al., *Oligodendrocyte-myelin glycoprotein is a Nogo receptor ligand that inhibits neurite outgrowth.* Nature, 2002. **417**(6892): p. 941-4.
8. Grados-Munro, E.M. and A.E. Fournier, *Myelin-associated inhibitors of axon regeneration.* Journal of Neuroscience Research, 2003. **74**(4): p. 479-85.
9. Bongiorno, D. and S. Petratos, *Molecular regulation of Nogo-A in neural cells: Novel insights into structure and function.* International Journal of Biochemistry & Cell Biology, 2010. **42**(7): p. 1072-1075.
10. Li, M.F. and J.X. Song, *The N- and C-termini of the human Nogo molecules are intrinsically unstructured: Bioinformatics, CD, NMR characterization, and functional implications.* Proteins-Structure Function and Bioinformatics, 2007. **68**(1): p. 100-108.
11. Schwab, M.E., *Functions of Nogo proteins and their receptors in the nervous system.* Nature Reviews Neuroscience, 2010. **11**(12): p. 799-811.
12. GrandPre, T., et al., *Identification of the Nogo inhibitor of axon regeneration as a Reticulon protein.* Nature, 2000. **403**(6768): p. 439-444.
13. McGee, A.W. and S.M. Strittmatter, *The Nogo-66 receptor: focusing myelin inhibition of axon regeneration.* Trends in Neurosciences, 2003. **26**(4): p. 193-198.
14. He, Z.G. and V. Koprivica, *The Nogo signaling pathway for regeneration block.* Annual Review of Neuroscience, 2004. **27**: p. 341-368.
15. Wang, X., et al., *Localization of Nogo-A and Nogo-66 receptor proteins at sites of axon-myelin and synaptic contact.* Journal of Neuroscience, 2002. **22**(13): p. 5505-15.
16. Fournier, A.E., et al., *Nogo and the Nogo-66 receptor.* Spinal Cord Trauma: Regeneration, Neural Repair and Functional Recovery, 2002. **137**: p. 361-369.
17. Domeniconi, M., et al., *Myelin-associated glycoprotein interacts with the Nogo66 receptor to inhibit neurite outgrowth.* Neuron, 2002. **35**(2): p. 283-290.
18. Lauren, J., et al., *Characterization of myelin ligand complexes with neuronal Nogo-66 receptor family members.* Journal of Biological Chemistry, 2007. **282**(8): p. 5715-25.

19. Barton, W.A., et al., *Structure and axon outgrowth inhibitor binding of the Nogo-66 receptor and related proteins.* Embo Journal, 2003. **22**(13): p. 3291-3302.
20. Hunt, D., et al., *Nogo receptor mRNA expression in intact and regenerating CNS neurons.* Molecular and Cellular Neuroscience, 2002. **20**(4): p. 537-552.
21. Wang, X.X., et al., *Localization of Nogo-A and Nogo-66 receptor proteins at sites of axon-myelin and synaptic contact.* Journal of Neuroscience, 2002. **22**(13): p. 5505-5515.
22. Atwal, J.K., et al., *PirB is a functional receptor for myelin inhibitors of axonal regeneration.* Science, 2008. **322**(5903): p. 967-70.
23. Wang, K.C., et al., *p75 interacts with the Nogo receptor as a co-receptor for Nogo, MAG and OMgp.* Nature, 2002. **420**(6911): p. 74-78.
24. Farinas, I., et al., *Characterization of neurotrophin and Trk receptor functions in developing sensory ganglia: direct NT-3 activation of TrkB neurons in vivo.* Neuron, 1998. **21**(2): p. 325-34.
25. Roux, P.P. and P.A. Barker, *Neurotrophin signaling through the p75 neurotrophin receptor.* Progress in Neurobiology, 2002. **67**(3): p. 203-33.
26. Satoh, J., et al., *TROY and LINGO-1 expression in astrocytes and macrophages/microglia in multiple sclerosis lesions.* Neuropathology and Applied Neurobiology, 2007. **33**(1): p. 99-107.
27. Cao, Z., et al., *Receptors for myelin inhibitors: Structures and therapeutic opportunities.* Molecular and Cellular Neuroscience, 2010. **43**(1): p. 1-14.
28. Mi, S., et al., *LINGO-1 is a component of the Nogo-66 receptor/p75 signaling complex.* Nature Neuroscience, 2004. **7**(3): p. 221-228.
29. Park, J.B., et al., *A TNF receptor family member, TROY, is a coreceptor with Nogo receptor in mediating the inhibitory activity of myelin inhibitors.* Neuron, 2005. **45**(3): p. 345-51.
30. Lee, X., et al., *NGF regulates the expression of axonal LINGO-1 to inhibit oligodendrocyte differentiation and myelination.* Journal of Neuroscience, 2007. **27**(1): p. 220-5.
31. Mi, S., et al., *LINGO-1 is a component of the Nogo-66 receptor/p75 signaling complex.* Nature Neuroscience, 2004. **7**(3): p. 221-8.
32. Ji, B., et al., *LINGO-1 antagonist promotes functional recovery and axonal sprouting after spinal cord injury.* Molecular and Cellular Neuroscience, 2006. **33**(3): p. 311-320.
33. Merenmies, J. and H. Rauvala, *Molecular cloning of the 18-kDa growth-associated protein of developing brain.* Journal of Biological Chemistry, 1990. **265**(28): p. 16721-4.
34. Chen, Y.N., et al., *AMIGO and friends: An emerging family of brain-enriched, neuronal growth modulating, type I transmembrane proteins with leucine-rich repeats (LRR) and cell adhesion molecule motifs.* Brain Research Reviews, 2006. **51**(2): p. 265-274.
35. Kuja-Panula, J., et al., *AMIGO, a transmembrane protein implicated in axon tract development, defines a novel protein family with leucine-rich repeats.* Journal of Cell Biology, 2003. **160**(6): p. 963-973.
36. Frentzel, S., et al., *Characterization of two novel proteins, NgRH1 and NgRH2, structurally and biochemically homologous to the Nogo-66 receptor.* Journal of Neurochemistry, 2003. **85**(3): p. 717-728.
37. Nardi, N.B., *All the adult stem cells, where do they all come from? An external source for organ-specific stem cell pools.* Med Hypotheses, 2005. **64**(4): p. 811-7.

38. Caplan, A.I. and S.P. Bruder, *Mesenchymal stem cells: building blocks for molecular medicine in the 21st century.* Trends in Molecular Medicine, 2001. **7**(6): p. 259-64.
39. Fuchs, E., T. Tumbar, and G. Guasch, *Socializing with the neighbors: stem cells and their niche.* Cell, 2004. **116**(6): p. 769-78.
40. Watt, F.M. and B.L. Hogan, *Out of Eden: stem cells and their niches.* Science, 2000. **287**(5457): p. 1427-30.
41. Bonnet, D., *Haematopoietic stem cells.* Journal of Pathology, 2002. **197**(4): p. 430-40.
42. Tocci, A. and L. Forte, *Mesenchymal stem cell: use and perspectives.* Hematol J, 2003. **4**(2): p. 92-6.
43. Phinney, D.G. and D.J. Prockop, *Concise review: mesenchymal stem/multipotent stromal cells: the state of transdifferentiation and modes of tissue repair--current views.* Stem Cells, 2007. **25**(11): p. 2896-902.
44. Vogel, W., et al., *Heterogeneity among human bone marrow-derived mesenchymal stem cells and neural progenitor cells.* Haematologica, 2003. **88**(2): p. 126-33.
45. Le Blanc, K., et al., *Mesenchymal stem cells inhibit and stimulate mixed lymphocyte cultures and mitogenic responses independently of the major histocompatibility complex.* Scandinavian Journal of Immunology, 2003. **57**(1): p. 11-20.
46. Dominici, M., et al., *Minimal criteria for defining multipotent mesenchymal stromal cells. The International Society for Cellular Therapy position statement.* Cytotherapy, 2006. **8**(4): p. 315-7.
47. da Silva Meirelles, L., A.I. Caplan, and N.B. Nardi, *In search of the in vivo identity of mesenchymal stem cells.* Stem Cells, 2008. **26**(9): p. 2287-99.
48. Tallone, T., et al., *Adult Human Adipose Tissue Contains Several Types of Multipotent Cells.* Journal of Cardiovascular Translational Research, 2011. **4**(2): p. 200-210.
49. Schipani, E. and H.M. Kronenberg, *Adult mesenchymal stem cells.* 2008.
50. Wexler, S.A., et al., *Adult bone marrow is a rich source of human mesenchymal 'stem' cells but umbilical cord and mobilized adult blood are not.* Br J Haematol, 2003. **121**(2): p. 368-74.
51. Bieback, K., et al., *Comparative analysis of mesenchymal stem cells from bone marrow, umbilical cord blood, or adipose tissue.* Stem Cells, 2006. **24**(5): p. 1294-1301.
52. Nardi, N.B., L.D.S. Meirelles, and P.C. Chagastelles, *Mesenchymal stem cells reside in virtually all post-natal organs and tissues.* Journal of Cell Science, 2006. **119**(11): p. 2204-2213.
53. Zuk, P.A., et al., *Human adipose tissue is a source of multipotent stem cells.* Molecular Biology of the Cell, 2002. **13**(12): p. 4279-95.
54. Feng, J.X., et al., *[Isolation of human pluripotent mesenchymal stem cells from second-trimester amniotic fluid using two kinds of culture protocol and their differentiation into neuron-like cells].* Zhongguo Wei Zhong Bing Ji Jiu Yi Xue, 2009. **21**(12): p. 729-33.
55. Gronthos, S., et al., *Postnatal human dental pulp stem cells (DPSCs) in vitro and in vivo.* Proc Natl Acad Sci U S A, 2000. **97**(25): p. 13625-30.
56. Young, H.E., et al., *Mesenchymal Stem-Cells Reside within the Connective Tissues of Many Organs.* Developmental Dynamics, 1995. **202**(2): p. 137-144.
57. Alm, J.J., et al., *Circulating plastic adherent mesenchymal stem cells in aged hip fracture patients.* Journal of Orthopaedic Research, 2010. **28**(12): p. 1634-42.

58. Zvaifler, N.J., et al., *Mesenchymal precursor cells in the blood of normal individuals.* Arthritis Research, 2000. **2**(6): p. 477-488.
59. Mansilla, E., et al., *Bloodstream cells phenotypically identical to human mesenchymal bone marrow stem cells circulate in large amounts under the influence of acute large skin damage: New evidence for their use in regenerative medicine.* Transplantation Proceedings, 2006. **38**(3): p. 967-969.
60. Pittenger, M.F. and S. Aggarwal, *Human mesenchymal stem cells modulate allogeneic immune cell responses.* Blood, 2005. **105**(4): p. 1815-1822.
61. Haynesworth, S.E., M.A. Baber, and A.I. Caplan, *Cytokine expression by human marrow-derived mesenchymal progenitor cells in vitro: effects of dexamethasone and IL-1 alpha.* J Cell Physiol, 1996. **166**(3): p. 585-92.
62. Le Blanc, K., et al., *Mesenchymal stem cells inhibit the expression of CD25 (interleukin-2 receptor) and CD38 on phytohaemagglutinin-activated lymphocytes.* Scandinavian Journal of Immunology, 2004. **60**(3): p. 307-315.
63. Maccario, R., et al., *Interaction of human mesenchymal stem cells with cells involved in alloantigen-specific immune response favors the differentiation of CD4+ T-cell subsets expressing a regulatory/suppressive phenotype.* Haematologica, 2005. **90**(4): p. 516-25.
64. Jiang, X.X., et al., *Human mesenchymal stem cells inhibit differentiation and function of monocyte-derived dendritic cells.* Blood, 2005. **105**(10): p. 4120-6.
65. Selmani, Z., et al., *Human leukocyte antigen-G5 secretion by human mesenchymal stem cells is required to suppress T lymphocyte and natural killer function and to induce CD4+CD25highFOXP3+ regulatory T cells.* Stem Cells, 2008. **26**(1): p. 212-22.
66. Plumas, J., et al., *Mesenchymal stem cells induce apoptosis of activated T cells.* Leukemia, 2005. **19**(9): p. 1597-604.
67. Tse, W.T., et al., *Suppression of allogeneic T-cell proliferation by human marrow stromal cells: implications in transplantation.* Transplantation, 2003. **75**(3): p. 389-97.
68. Noel, D., et al., *Immunosuppressive effect of mesenchymal stem cells favors tumor growth in allogeneic animals.* Blood, 2003. **102**(10): p. 3837-3844.
69. Waterman, R.S., et al., *A new mesenchymal stem cell (MSC) paradigm: polarization into a pro-inflammatory MSC1 or an Immunosuppressive MSC2 phenotype.* Plos One, 2010. **5**(4): p. e10088.
70. Le Blanc, K., *Immunomodulatory effects of fetal and adult mesenchymal stem cells.* Cytotherapy, 2003. **5**(6): p. 485-489.
71. von Bonin, M., et al., *Treatment of refractory acute GvHD with mesenchymal stem cells: organ-specific responses and outcomes.* Bone Marrow Transplantation, 2008. **41**: p. S232-S233.
72. Amado, L.C., et al., *Cardiac repair with intramyocardial injection of allogeneic mesenchymal stem cells after myocardial infarction.* Proc Natl Acad Sci U S A, 2005. **102**(32): p. 11474-9.
73. Horwitz, E.M., et al., *Clinical responses to bone marrow transplantation in children with severe osteogenesis imperfecta.* Blood, 2001. **97**(5): p. 1227-31.
74. Marino, R., et al., *Transplantable marrow osteoprogenitors engraft in discrete saturable sites in the marrow microenvironment.* Experimental Hematology, 2008. **36**(3): p. 360-8.
75. Gao, J., et al., *The dynamic in vivo distribution of bone marrow-derived mesenchymal stem cells after infusion.* Cells Tissues Organs, 2001. **169**(1): p. 12-20.

76. Horwitz, E.M., et al., *Isolated allogeneic bone marrow-derived mesenchymal cells engraft and stimulate growth in children with osteogenesis imperfecta: Implications for cell therapy of bone.* Proc Natl Acad Sci U S A, 2002. **99**(13): p. 8932-7.
77. Ortiz, L.A., et al., *Mesenchymal stem cell engraftment in lung is enhanced in response to bleomycin exposure and ameliorates its fibrotic effects.* Proceedings of the National Academy of Sciences of the United States of America, 2003. **100**(14): p. 8407-8411.
78. Fox, J.M., et al., *Recent advances into the understanding of mesenchymal stem cell trafficking.* Br J Haematol, 2007. **137**(6): p. 491-502.
79. Langer, H.F., et al., *Platelet derived bFGF mediates vascular integrative mechanisms of mesenchymal stem cells in vitro.* Journal of Molecular and Cellular Cardiology, 2009. **47**(2): p. 315-25.
80. Ruster, B., et al., *Mesenchymal stem cells display coordinated rolling and adhesion behavior on endothelial cells.* Blood, 2006. **108**(12): p. 3938-44.
81. Caplan, A.I. and J.E. Dennis, *Mesenchymal stem cells as trophic mediators.* Journal of Cellular Biochemistry, 2006. **98**(5): p. 1076-84.
82. Doucet, C., et al., *Platelet lysates promote mesenchymal stem cell expansion: a safety substitute for animal serum in cell-based therapy applications.* J Cell Physiol, 2005. **205**(2): p. 228-36.
83. Anitua, E., et al., *Autologous platelets as a source of proteins for healing and tissue regeneration.* Thromb Haemost, 2004. **91**(1): p. 4-15.
84. Weyrich, A.S. and G.A. Zimmerman, *Platelets: signaling cells in the immune continuum.* Trends Immunol, 2004. **25**(9): p. 489-95.
85. Gawaz, M., et al., *Activated platelets induce monocyte chemotactic protein-1 secretion and surface expression of intercellular adhesion molecule-1 on endothelial cells.* Circulation, 1998. **98**(12): p. 1164-1171.
86. Massberg, S. and U.H. von Andrian, *Novel Trafficking Routes for Hematopoietic Stem and Progenitor Cells.* Hematopoietic Stem Cells Vii, 2009. **1176**: p. 87-93.
87. Janowska-Wieczorek, A., et al., *Platelet-derived microparticles bind to hematopoietic stem/progenitor cells and enhance their engraftment.* Blood, 2001. **98**(10): p. 3143-9.
88. Frenette, P.S., et al., *Endothelial selectins and vascular cell adhesion molecule-1 promote hematopoietic progenitor homing to bone marrow.* Proc Natl Acad Sci U S A, 1998. **95**(24): p. 14423-8.
89. Massberg, S., et al., *Activated platelets trigger an inflammatory response and enhance migration of aortic smooth muscle cells.* Thrombosis Research, 2003. **110**(4): p. 187-194.
90. McNicol, A. and C.A. Robson, *Thrombin receptor-activating peptide releases arachidonic acid from human platelets: a comparison with thrombin and trypsin.* Journal of Pharmacology and Experimental Therapeutics, 1997. **281**(2): p. 861-7.